

## **General Disclaimer**

### **One or more of the Following Statements may affect this Document**

- This document has been reproduced from the best copy furnished by the organizational source. It is being released in the interest of making available as much information as possible.
- This document may contain data, which exceeds the sheet parameters. It was furnished in this condition by the organizational source and is the best copy available.
- This document may contain tone-on-tone or color graphs, charts and/or pictures, which have been reproduced in black and white.
- This document is paginated as submitted by the original source.
- Portions of this document are not fully legible due to the historical nature of some of the material. However, it is the best reproduction available from the original submission.

G3/44      Unclass  
21046

**FINAL TECHNICAL PROGRESS REPORT**  
**FOR THE**  
**DEVELOPMENT OF ADVANCED THERMOELECTRIC MATERIALS**

**1 October 1975 to 31 January 1984**  
**Contract Number 954349**

**TE380-53-84**



Prepared for  
Jet Propulsion Laboratory  
Pasadena, CA

Prepared by  
Thermo Electron Corporation  
Waltham, Massachusetts

This work was performed for the Jet Propulsion Laboratory, California Institute of Technology sponsored by the National Aeronautics and Space Administration under Contract NAS 7-918

## TABLE OF CONTENTS

	<u>Page</u>
I. INTRODUCTION . . . . .	1
II. IMPROVED SILICON-GERMANIUM ALLOYS . . . . .	2
III. LANTHANUM CHROME SULFIDE . . . . .	23
IV. CHROME SULFIDE AND LANTHANUM SULFIDE . . . . .	35
V. SUMMARY . . . . .	52

## LIST OF ILLUSTRATION

<u>Figure</u>	<u>Page</u>
Figure 1 - Absolute Seebeck Coefficient of Various Samples of Silicon-Germanium Alloys with Gallium Phosphide Additions . . . . .	11
Figure 2 - Thermal Conductivities of Various Samples of Silicon-Germanium Alloys with Gallium Phosphide Additions . . . . .	13
Figure 3 - Electrical Resistivities of Various Samples of Silicon-Germanium Alloys with Gallium Phosphide Additions . . . . .	17
Figure 4 - Changes in Electrical Resistivities of Various Silicon-Germanium Alloys with Gallium Phosphide Additions as a Result of Annealing . . . . .	19
Figure 5 - The Figures-of-Merit of a Silicon-Germanium Alloy and the Same Alloy Modified with Gallium Phosphide Addition . . .	21
Figure 6 - Weight Loss Characteristics of Various Thermoelectric Materials . . . . .	22
Figure 7 - High Temperature Thermoelectric Property Measurements Apparatus . . . . .	29
Figure 8 - Electrical Resistivities of $\text{LaCrS}_3$ as a Function of Annealing . . . . .	31
Figure 9 - Absolute Seebeck Coefficient of $\text{LaCrS}_3$ as a Function of Annealing . . . . .	32
Figure 10 - Power Factors of $\text{LaCrS}_3$ as a Function of Annealing . . . . .	34
Figure 11 - Temperature Dependence of the Thermal Conductivity of $(\text{La}_2\text{S}_3)_{1-x}(\text{Cr}_2\text{S}_3)_x$ Solid Solutions . . . . .	37
Figure 12 - Temperature Dependence of the Electrical Resistivity of $(\text{La}_2\text{S}_3)_{0.75}(\text{Cr}_2\text{S}_3)_{0.25}$ . . . . .	37
Figure 13 - Temperature Dependence of the Electrical Resistivity of $(\text{La}_2\text{S}_3)_{1-x}(\text{Cr}_2\text{S}_3)_x$ Solid Solutions . . . . .	38

	<u>Page</u>
Figure 14 - Seebeck Coefficient of $(\text{La}_2\text{S}_3)_{1-x}(\text{Cr}_2\text{S}_3)_x$ Solid Solutions . . . . .	38
Figure 15 - Figure-of-Merit of $(\text{La}_2\text{S}_3)_{0.75}(\text{Cr}_2\text{S}_3)_{0.25}$ as a Function of Annealing . . . . .	40
Figure 16 - Figures-of-Merit of Various Mixtures of $\text{La}_2\text{S}_3$ and $\text{Cr}_2\text{S}_3$ After Annealing . . . . .	41
Figure 17 - Electrical Resistivity of $(\text{La}_2\text{S}_3)_{0.75}(\text{Cr}_2\text{S}_3)_{0.25}$	43
Figure 18 - Absolute Seebeck Coefficient of $(\text{La}_2\text{S}_3)_{0.75}(\text{Cr}_2\text{S}_3)_{0.25}$ . . . . .	44
Figure 19 - Lattice Thermal Conductivities of Various Mixtures of $\text{La}_2\text{S}_3$ and $\text{Cr}_2\text{S}_3$ . . . . .	46
Figure 20 - Carrier Concentration of $(\text{La}_2\text{S}_3)_{0.75}(\text{Cr}_2\text{S}_3)_{0.25}$	49
Figure 21 - Carrier Mobility of $(\text{La}_2\text{S}_3)_{0.75}(\text{Cr}_2\text{S}_3)_{0.25}$ . . . . .	51

## ABSTRACT

This report summarizes the work performed by the Thermo Electron Corporation on JPL Contract No. 954349 for the development of an advanced thermoelectric material for Radioisotope Thermoelectric Generator (RTG) applications. Although a number of materials were explored on the program, the bulk of the effort, as described in this report, was devoted to improving silicon-germanium alloys by the addition of gallium phosphide, the synthesis and evaluation of lanthanum chrome sulfide and the formulation of various mixtures of lanthanum sulfide and chrome sulfide. It was found that each of these materials exhibits promise as a thermoelectric material for the stated purpose.

## **I. INTRODUCTION**

This is the final report for the development of advanced thermoelectric materials on contract to the Jet Propulsion Laboratory, Contract No. 954349.

The efforts on the contract initially concerned themselves with attempts to improve silicon-germanium alloys by the alloying of silicides and germanides and by the addition of small quantities of III-V compounds. Subsequent efforts were devoted to investigations of various sulfides and alloys of sulfides.

Two promising improved thermoelectric materials were identified, but not fully developed on the program. The first of these is an improved silicon-germanium alloy with small additions of gallium phosphide. The second promising material is lanthanum chrome sulfide. The primary reason that both materials show promise as thermoelectric materials is that both exhibit low values of thermal conductivity, whereas their electrical properties are quite similar to other thermoelectric materials; the performance of a thermoelectric material is proportional to the inverse of the thermal conductivity of the material.

Although a variety of materials in addition to silicon-germanium alloys with gallium phosphide additions and lanthanum chrome sulfide were investigated on the program, none of the other materials showed promise as good thermoelectric materials. For this reason, the present report is devoted to a summary of the efforts on silicon-germanium alloys with gallium phosphide additives and lanthanum chrome sulfide.

## II. IMPROVED SILICON-GERMANIUM ALLOYS

Silicon-germanium alloys are capable of operation at temperatures up to 1000°C. A comparison of all available thermoelectric materials indicates that they possess the best mechanical and physical properties of any material. However, the figure-of-merit values of these alloys are lower than those of most other thermoelectric materials. Inasmuch as silicon-germanium alloys are capable of operation over greater temperature differentials than most other thermoelectric materials and inasmuch as conversion efficiency is proportional to the product of temperature differential and figure-of-merit, the relatively low values of figure-of-merit of silicon-germanium alloys are compensated and conversion efficiencies available with these alloys are comparable to those available with most other thermoelectric materials. On the other hand, if it were possible to substantially improve the figure-of-merit of silicon-germanium alloys without affecting their other characteristics, the result would be a thermoelectric material that would be better than any other presently available material.

An inspection of the properties that make up the figure-of-merit indicates that it is primarily the relatively high thermal conductivity of silicon-germanium alloys that results in the low figure-of-merit, when compared to other thermoelectric materials. Thermal conductivity consists of various components with the lattice component generally predominating in most thermoelectric materials. Lattice



thermal conductivity  $\kappa$ , be decreased by increasing phonon scattering. In the case of silicon-germanium alloys, this has been achieved by forming solid solutions of silicon and germanium<sup>1</sup>. Introducing more disorder in the lattice by the addition of impurity atoms, creation of vacancies at lattice sites, introduction of defects and increasing the atomic weight of the lattice components are some of the methods by which the thermal conductivity can be further reduced. However, reduction of thermal conductivity by these methods frequently results in increased electron scattering and consequently an increase in the electrical resistivity. Thus, any increase in the electrical resistivity must be over compensated by a reduction in thermal conductivity, if the figure-of-merit of a material is to be improved.

Because Group III and V elements are compatible with silicon and germanium and because electron mobilities of III-V compounds are much higher than those of silicon-germanium alloys, it has been considered that the addition of small amounts of Group III-V compounds to silicon-germanium alloys may improve their figures-of-merit. Gallium phosphide is isostructural and isoelectronic with silicon-germanium alloys, and it has lower values of vapor pressure than other Group III-V compounds at high temperatures. Therefore, the preliminary efforts in the modification of silicon-germanium alloys have been directed to the addition of small amounts of gallium phosphide.

Alloys of 50 a/o Si - 50 a/o Ge and 63 a/o Si - 37 a/o Ge were prepared by placing precisely weighed quantities of the elements in a quartz crucible and melting them in vacuum. P-type and n-type materials were prepared by the addition of boron and phosphorus, respectively. The melted material was subsequently etched with HF-HNO<sub>3</sub> and then pulverized and thoroughly blended with the desired amount of gallium phosphide. The uniform mixture was then hot pressed in vacuum at 1000°C. In this manner, cylindrical pellets with 92 to 97 percent of theoretical density were obtained.

The pellets were then sealed in evacuated quartz ampules with small amounts of excess phosphorus. The excess phosphorus was added in order to prevent the thermal decomposition of gallium phosphide during the subsequent annealing cycle. The pellets were annealed at 1000°C for ten days to complete the diffusion of gallium phosphide into the silicon-germanium alloys. The sintered pellets were then subjected to thermoelectric property measurements.

Electrical resistivities of the pellets were measured by means of direct current, four probe method. Each pellet was mounted in an apparatus which can be used for measuring Seebeck coefficient, thermal conductivity and electrical resistivity simultaneously as a function of temperature. The details of the apparatus are given elsewhere<sup>2</sup>. During measurement, the whole apparatus is maintained in an evacuated chamber, with current probes and thermocouple lead wires positioned on each sample within precisely drilled microholes along the length of

the sample. This assures good contact between the sample and the lead wires. Electrical resistivity measurements were corrected for contributions of the Seebeck voltage by alternating the direction of current flow.

Hall coefficient measurements were performed on rectangular slices of a thickness of about 0.005 inch. Gold wires were bonded to each sample by means of a silver conducting paste. Because of thermal noise, an a.c. method was used with a PAR lock-in amplifier for signal measurements. Each sample was placed in the field of an electromagnet with a variable field strength of up to 6000 Gauss. Hall voltages were measured at various field strengths in both field directions. An alloy of silicon-germanium of known doping level was used to check the accuracy of the results. No magneto-resistance was found at room temperature and no correction to the Hall voltage was therefore necessary.

Thermal conductivity values of the cylindrical test pellets were measured using a steady state comparison method of longitudinal heat flow. Experimental details were described elsewhere<sup>3</sup>. Pyroceram cylinders were used as standards. The accuracy of the measurements was determined by means of measurements of several standard materials of known thermal conductivity. It was found that the accuracy of the measurement is approximately  $\pm$  five percent at temperatures below 500°C. The accuracy of measurements at higher temperatures is lower than that because of the radiation loss inherent in this type of measurement. The temperature gradient

along the sample at the steady state conditions was measured by thermocouples placed in microholes drilled into the test pellets; prior to each measurement, sufficient time was allowed to attain temperature equilibrium.

Even though both gallium and phosphorus have very low solid solubilities (less than one atomic percent) in silicon and germanium, it has been found here as well as earlier<sup>4,5</sup> that cross-doping increase the solid solubility. Glazove and Zemskov<sup>5</sup> have found marked maxima in the solid solubilities of Group III-V compounds in silicon and germanium. Frequently, solids with similar crystal structures and bonding characteristics and having lattice parameters not very different from one another show mutual solid solubility. The solid solubility is sometimes limited because of the excess distortion of the chemical bonds that result from the differences in the electronegativities of the elements. When two or more components are introduced, chemical interaction may lead to phase separation.

Table 1 lists some of the physical parameters of Group III-V compounds along with those of silicon and germanium. From the table, it is seen that both gallium phosphide and gallium arsenide are isostructural with silicon and germanium and that their lattice parameters are very close to those of silicon and germanium. It is therefore not surprising that these compounds show some mutual solid solubility. Complete formation of solid solutions or a large solid solubility is not possible because of the large difference in the ionicity of bonding.

TABLE 1

Comparison of the Room Temperature Properties of  
Selected Undoped Group IV and Group III-V Elements and Compounds

Element Compounds	Thermal Conductivity watt/°C-cm	$\Delta E$ eV	$\mu_e \times 10^{-3}$ cm <sup>2</sup> /v-sec (N)	$\mu_p \times 10^{-3}$ cm <sup>2</sup> /v-sec (P)	Lattice Constant Å°	Melting Point °C	Molecular Weight
Si	1.50	1.21	1.45	0.50	5.43	1420	28.086
Ge	0.78	0.78	3.80	3.00	5.62	937	72.590
Si <sub>0.5</sub> Ge <sub>0.5</sub>	0.08	1.05	0.20	0.10	5.55	1100	50.330
Si <sub>0.63</sub> Ge <sub>0.37</sub>	0.08	1.10	0.20	0.10	5.51	1175	55.570
GaP	0.80	2.20	0.30	0.15	5.44	1350	100.690
GaAs	0.40	1.40	7.00	0.20	5.63	1240	144.64

It has been known that one of the factors which limits the solid solubility of Group III and Group V elements in silicon and germanium is the creation of vacancies. Therefore, when both Group III and Group V elements are incorporated in silicon and germanium in equal amounts, creation of such vacancies is minimized and the mechanism of the formation of a solid solution is favored. If Group III and Group V elements are not introduced in an equal atomic ratio in the host matrix, the solid solubility of each element is decreased. The present experimental results, as well as the results of others<sup>5</sup>, clearly indicate this to be the case.

The present work has not considered the introduction of gallium phosphide or gallium arsenide into pure silicon and germanium, but rather into silicon-germanium alloys because the primary interest has been the reduction of the thermal conductivity of the alloys. It should be noted that the consideration of the solid solubility of Group III and Group V elements in silicon and germanium is directly applicable also to the silicon-germanium alloys because silicon and germanium form a continuous range of solid solutions.

It has been found that the maximum solid solubility of gallium phosphide in silicon-germanium alloys achieved by solid state sintering is about five to eight atomic percent. Formation of one uniform phase of silicon-germanium alloys with gallium phosphide can be obtained only after prolonged annealing in vacuum at 1000°C, as it involves a solid state diffusion mechanism. The particle size of the constituent

materials is important in controlling the rate of diffusion. Because of very slow diffusion rates, it has not been possible to obtain a uniform phase when the particle size exceeds 180 microns. Even though solid solutions are usually formed by the simultaneous melting of the individual components, such a procedure was not successful in the present case because of the thermal decomposition of gallium phosphide at the melting points of silicon-germanium alloys. X-ray powder diffraction and electron microprobe analyses were used to characterize all materials.

Thermoelectric properties of p-type 50 a/o Si - 50 a/o Ge + 8 m/o GaP and n- and p-type 63 a/o Si - 37 a/o Ge + 8 m/o GaP, as well as of n-type 63 a/o Si - 37 a/o Ge + 4 m/o GaP were measured by the methods discussed above. Representative samples subjected to measurement are identified in Table 2. The absolute Seebeck coefficient values of these samples are shown in Figure 1 as a function of temperature. The Seebeck coefficient values shown in Figure 1 indicate that the addition of gallium phosphide to silicon-germanium alloys does not have a significant effect on the Seebeck coefficient values, even though these values are slightly decreased in the n-type material and slightly increased in the p-type material. It is believed that the reason for this phenomenon is not the addition of gallium phosphide to the alloys but rather the slight doping effect experienced by the material during its anneal in a phosphorus atmosphere after its preparation. Any diffusion of phosphorus into the material would tend to

TABLE 2

Identification of Samples Represented by Data in Figures 1 to 5

<u>Sample No.</u>	<u>Ratio of Si to Ge</u>	<u>% GaP m/o</u>	<u>Particle Size-<math>\mu</math></u>	<u>Polarity</u>
1	50/50	8	<44	p
2	63/37	8	<44	p
3	63/37	8	<44	n
4	63/37	0	180	n
5	63/37	0	180	p
6	63/37	8	180-300	n
7	63/37	4	180-300	n
8	63/37	8	44-80	n



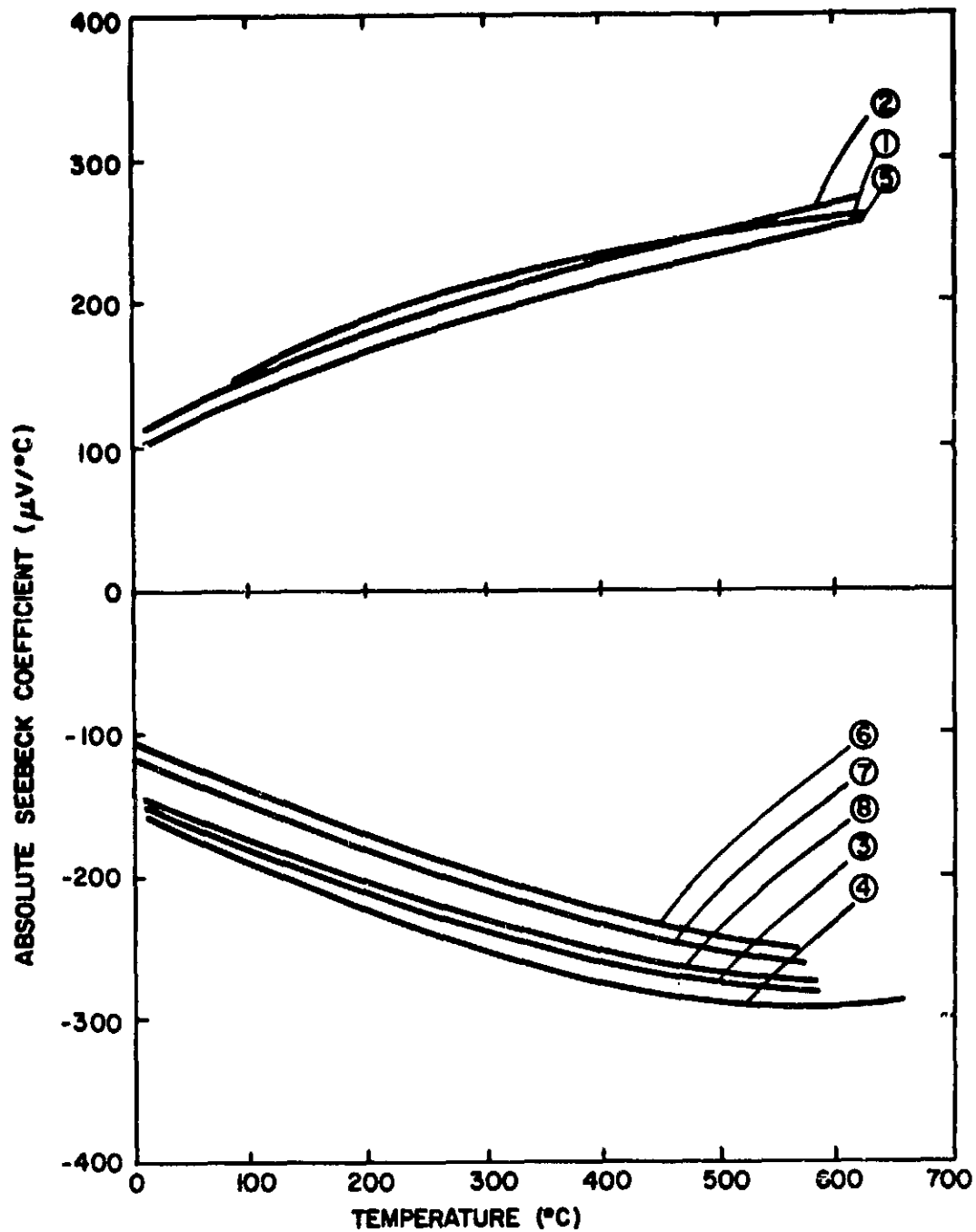


Figure 1. Absolute Seebeck Coefficients of Various Samples of Silicon-Germanium Alloys with Gallium Phosphide Additions. Samples are Identified by Number in Table 2.

enhance the doping of the n-type material and reduce the doping of the p-type material because of cross-doping. The results of such doping changes would be exactly what is observed in the Seebeck coefficient values in Figure 1. Although not known from experience, it may be postulated that these doping effects are reversible and that the Seebeck coefficient values of the material containing gallium phosphide would approach those of the material not containing gallium phosphide upon prolonged heating in vacuum.

The thermal conductivity values of various samples of silicon-germanium alloys with gallium phosphide additions are shown in Figure 2. It is noted in Figure 2 that a significant reduction occurs in the thermal conductivity of silicon-germanium alloys when small amounts of gallium phosphide are added to these alloys. A careful inspection of the figure furthermore indicates that in order for the gallium phosphide addition to have the desired effect on thermal conductivity, it is necessary that the material be prepared from very fine particle size starting material. The reason for this is that the thermal conductivity reduction occurs only if adequate interdiffusion of gallium phosphide and silicon-germanium takes place during material preparation and the resultant material consists of a single phase. In the case of material prepared from large size particles, it is noted that little reduction in thermal conductivity is experienced, even though the temperature dependence of the thermal conductivity is somewhat altered. The reason for this occurrence is that inadequate

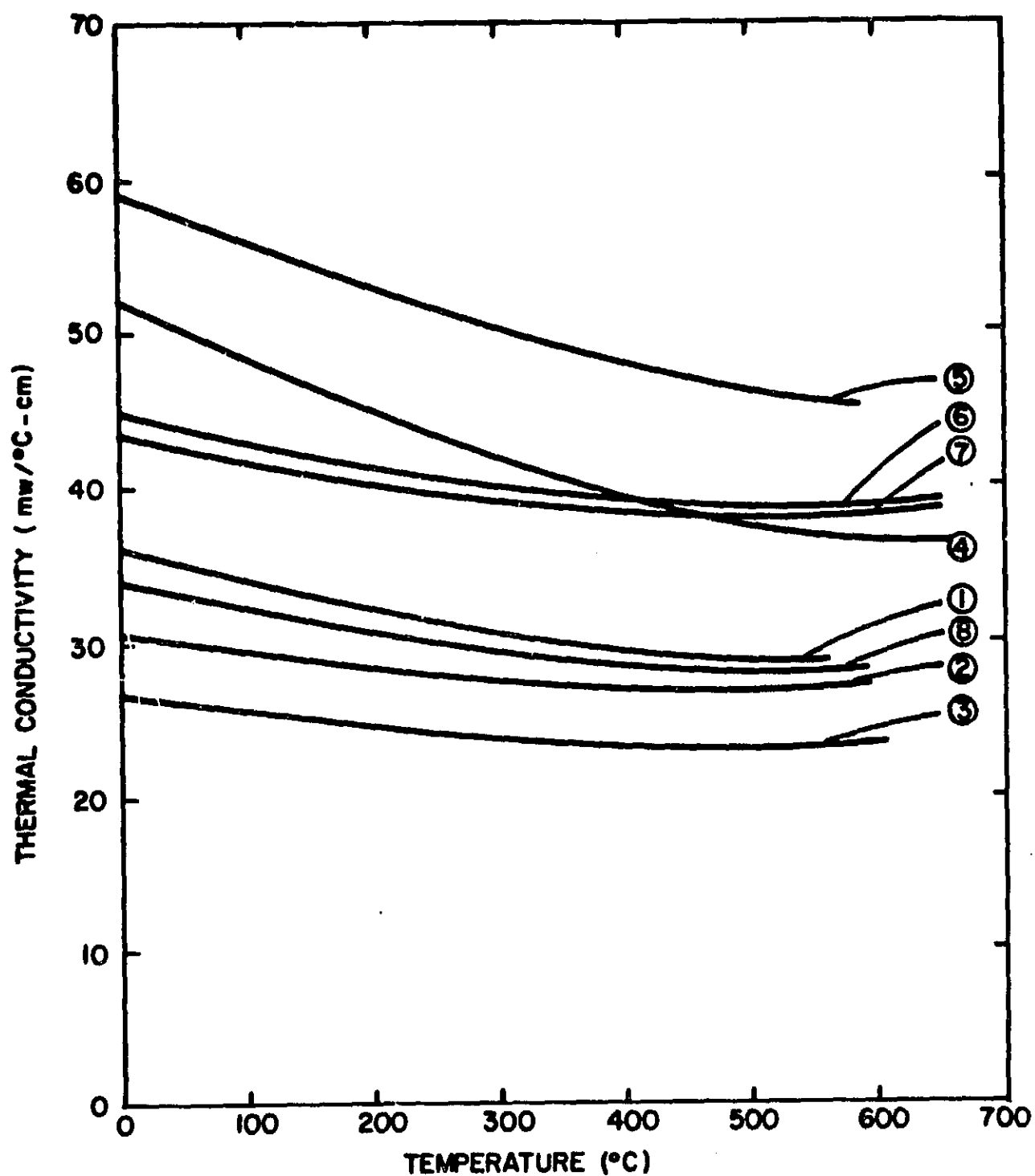


Figure 2. Thermal Conductivities of Various Samples of Silicon-Germanium Alloys with Gallium Phosphide Additions. Samples are Identified by Number in Table 2.

interdiffusion of gallium phosphide and silicon-germanium takes place during material preparation and the resultant material consists of two phases, with each phase having a thermal conductivity that is fairly high. It is further noted in Figure 2 that little difference exists in the thermal conductivity of silicon-germanium alloys with gallium phosphide additions when the gallium phosphide content is varied between four and eight molecular percent. From experiment it is known that the minimum thermal conductivity for the material with a gallium phosphide addition occurs in this range and that the thermal conductivity exhibits a broad minimum. However, it is also known that gallium phosphide concentrations outside of this range will result in rapidly increasing values of thermal conductivity. In the case of greater concentrations of gallium phosphide, the result is a two phase alloy in which the second phase possesses a fairly high thermal conductivity. In the case of smaller concentrations, inadequate amounts of gallium phosphide are used to attain minimum values of thermal conductivity.

It should be noted that most of the samples prepared and measured on the program had densities of the order of 92 to 97 percent of theoretical. It is recognized that a less than theoretical density may itself have a reducing effect on thermal conductivity. Analytical and experimental considerations, however, shown that such an effect can account for only some ten to 15 percent reduction in thermal conductivity. In Figure 2 it is seen that thermal conductivity

reductions of the order of 40 to 50 percent have been achieved. It is therefore concluded that most of the thermal conductivity reduction is due to the addition of gallium phosphide. Moreover, the fact that material prepared from large size particles exhibits thermal conductivity values very close to those of silicon-germanium alloys with theoretical density, even though these samples themselves are considerably less dense than theoretical, supports this conclusion. Finally, it should be mentioned that the reason for the relatively low density of the samples depicted in Figures 1 and 2 is the low pressing temperature used. More dense material may be made by pressing at higher temperatures. This can be accomplished under a phosphorus atmosphere without causing decomposition of gallium phosphide during pressing.

It has been found that the electrical resistivity of silicon-germanium alloys with gallium phosphide additions possesses generally higher values than those of corresponding silicon-germanium alloys in the as-prepared state. On the other hand, it has also been found that high temperature annealing significantly reduces electrical resistivity and after long annealing times appears to result in values quite comparable to those of silicon-germanium alloys. However, inasmuch as considerable variation exists between different samples even after annealing, it is recognized that considerable effort is still required to fully understand the process extant during annealing. The values of electrical resistivity representative test samples previously discussed in

connection with the results of Seebeck coefficient and thermal conductivity measurements are shown as a function of temperature in Figure 3. It is noted in connection with Figure 3 that all of the data, except those of the silicon-germanium alloys, pertain to samples that have undergone annealing at 1000°C for several hundred hours. It is noted that in some cases values of electrical resistivity quite comparable to those of silicon-germanium alloys are obtained. On the other hand, significantly higher values are also noted. Although electrical resistivity generally decreases with increasing particle size, this is not necessarily the case and, in fact, low values of electrical resistivity are also noted for samples prepared from very small particle size starting material. The higher than expected values of electrical resistivity for single phase samples may be due to a variety of reasons:

1. Reduced mobility of electrons due to the additional scattering by gallium and phosphorus atoms in the material.
2. Presence of oxides formed during hot pressing, because of the air trapped among the fine particles.
3. Inhomogeneity of the material.

It is noted that density is not considered to be a primary contributing factor to high values of electrical resistivity because density, unlike electrical resistivity, is not generally affected by annealing and does not appear to depend on the particle size of the starting material, as does

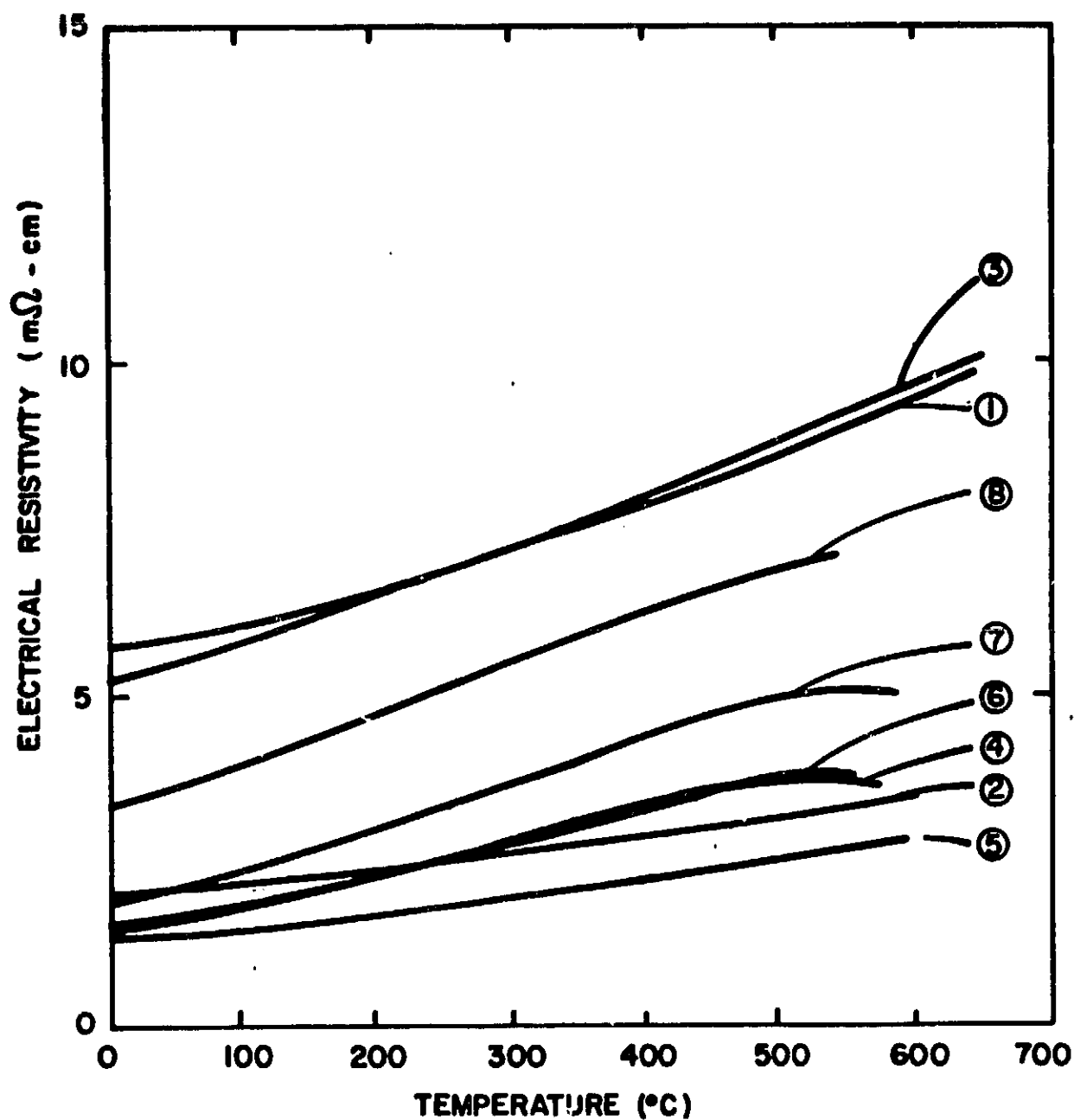


Figure 3. Electrical Resistivities of Various Samples of Silicon-Germanium Alloys with Gallium Phosphide Additions. Samples are Identified by Number in Table 2.

electrical resistivity. On the other hand, it is possible that the less than theoretical density of the material may limit the final values of electrical resistivity obtained after long annealing times.

The effect of annealing on the electrical resistivity of representative test samples is illustrated in Figure 4 in terms of electrical resistivity as a function of temperature. The annealing of the test samples underlying the data in Figure 4 was performed in vacuum at 950°C. Although annealing generally results in reduced electrical resistivity, it is noted in Figure 4 that the results are not uniform. Because of the non-uniformity of results, investigations are suggested to be conducted in order to obtain a better understanding of the annealing process. It is expected that this will result in the consistent ability to produce silicon-germanium alloys with gallium phosphide additions in which the electrical resistivity is essentially the same as that of silicon-germanium alloys. Finally, note is made of the fact that annealing of the material does not have any noticeable affect on the thermal conductivity of the material. A slight annealing effect is noticed on values of Seebeck coefficient; these values tend to approach those of silicon-germanium alloys of comparable doping level.

Most of the effort devoted on the addition of gallium phosphide to silicon-germanium alloys was devoted to the p-type material. Because of the greater emphasis, it has been possible to prepare p-type material with relatively higher



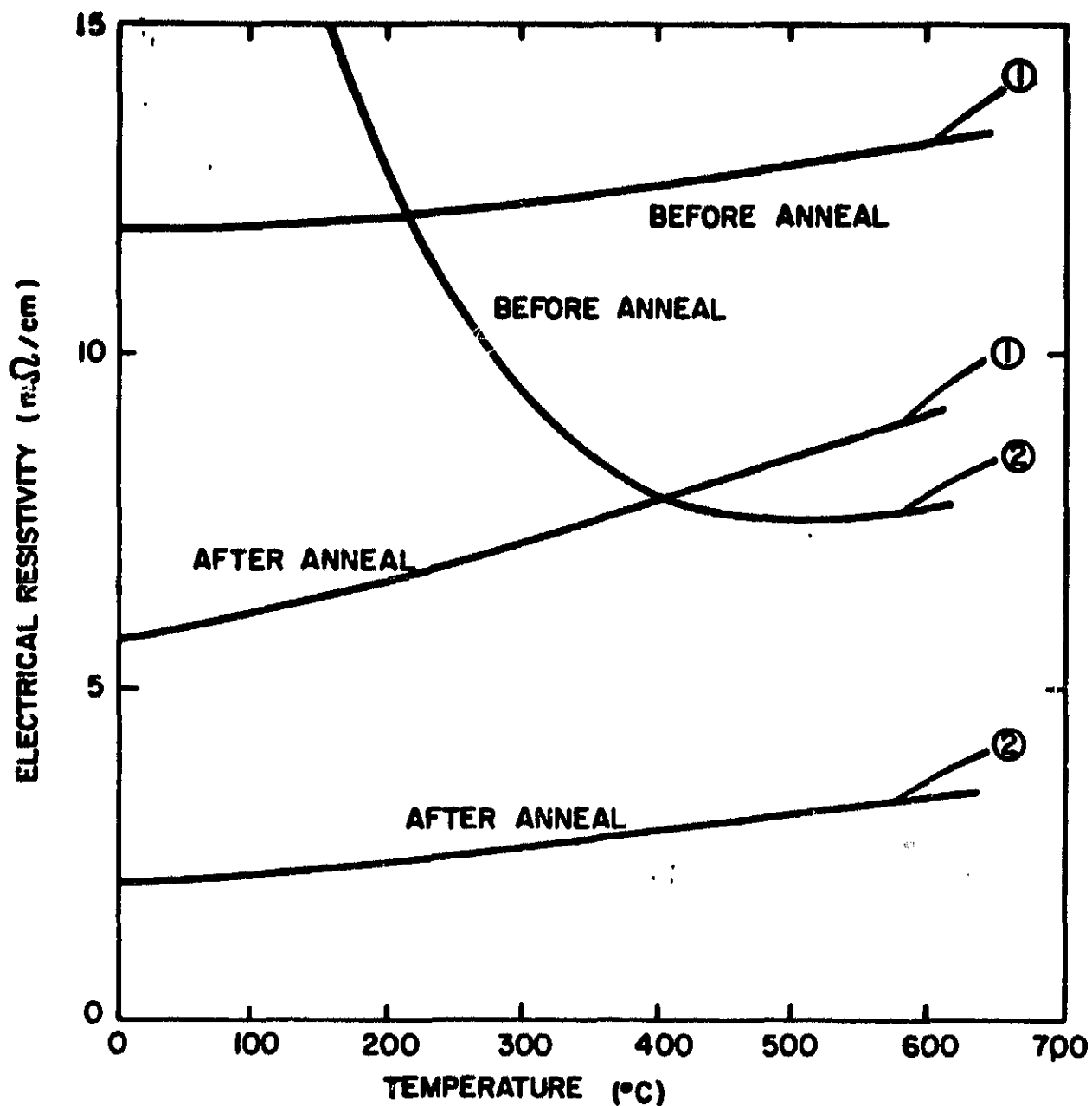


Figure 4. Changes in Electrical Resistivities of Various Silicon-Germanium Alloys with Gallium Phosphide Additions as a Result of Annealing. Samples are Identified by Number in Table 2.

values of figure-of-merit than the n-type material. Nevertheless, samples of both types of material with gallium phosphide additions have been prepared with figure-of-merit values higher than those of corresponding silicon-germanium alloys. This is illustrated by a plot of figure-of-merit as a function of temperature for the p-type alloy in Figure 5. It is noted that an average increase of about 25 percent in figure-of-merit has been obtained as a result of the addition of gallium phosphide to the 63 a/o Si - 37 a/o Ge alloy. It must be emphasized that it is projected that upon complete process optimization, the enhancement of figure-of-merit shown in Figure 5 can be considerably further increased. Moreover, comparable improvements in the figure-of-merit of the n-type material may be projected.

The sublimation of silicon-germanium alloys with gallium phosphide additions has been investigated by means of weight loss studies and the results are shown in Figure 6 in terms of the weight loss of the 50 a/o Si - 50 a/o Ge + 8 m/o GaP alloy as a function of inverse temperature. As anticipated, the weight loss of the 50 a/o Si - 50 a/o Ge + 8 m/o GaP alloy is higher than that of the 80 a/o Si - 20 a/o Ge alloy, also shown in Figure 6. However, the weight loss is dependent on alloy composition; the higher is the germanium content of the alloy, the higher is its weight loss. The results show good agreement with weight loss rates of alloys with corresponding silicon content<sup>7</sup>. It is thus concluded that the addition of gallium phosphide to silicon-germanium alloys does not affect their weight loss characteristics in any substantial way.

83-384

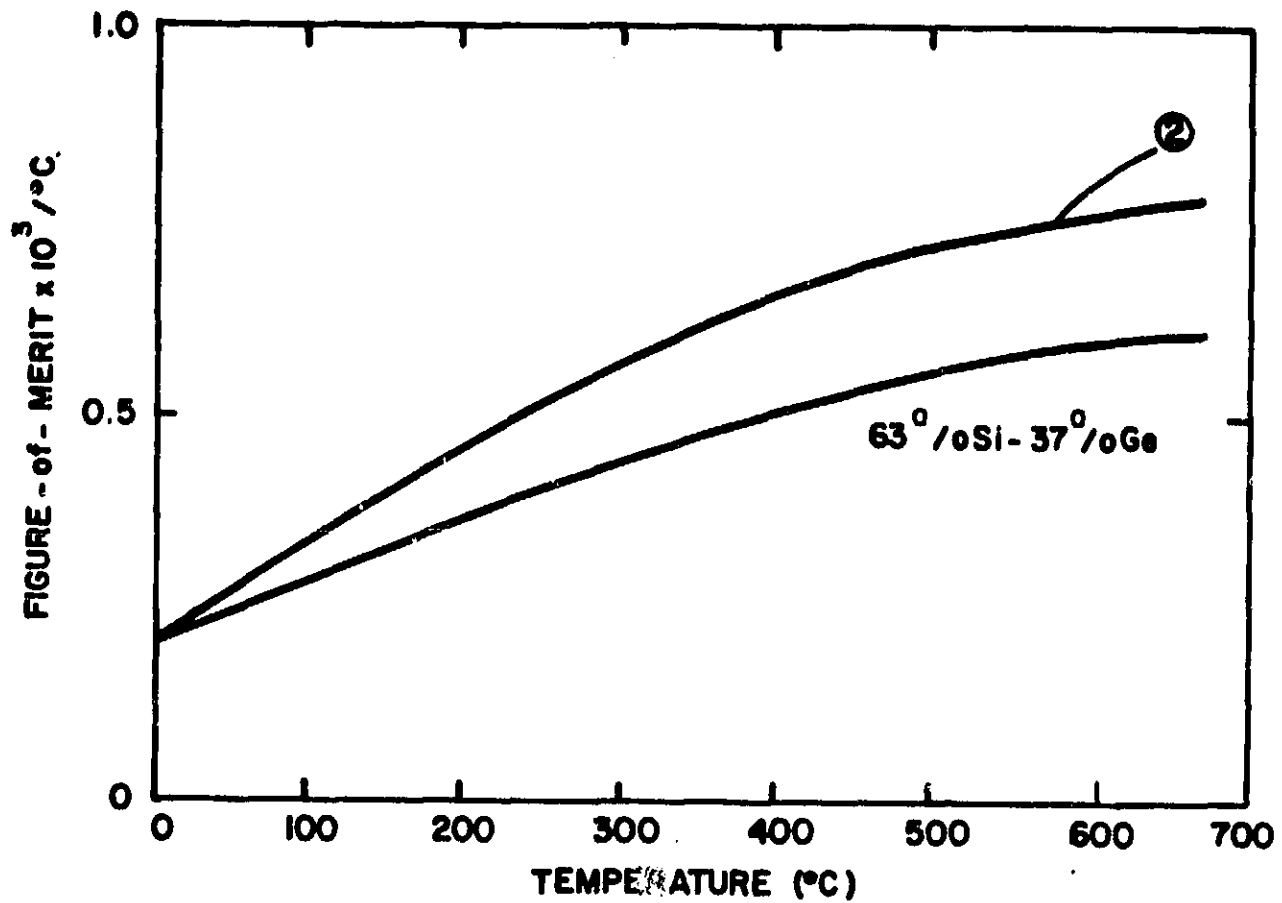


Figure 5. The Figures-of-Merit of a Silicon-Germanium Alloy and the Same Alloy Modified with Gallium Phosphide Addition. The Latter Material is Identified by Number in Table 2.

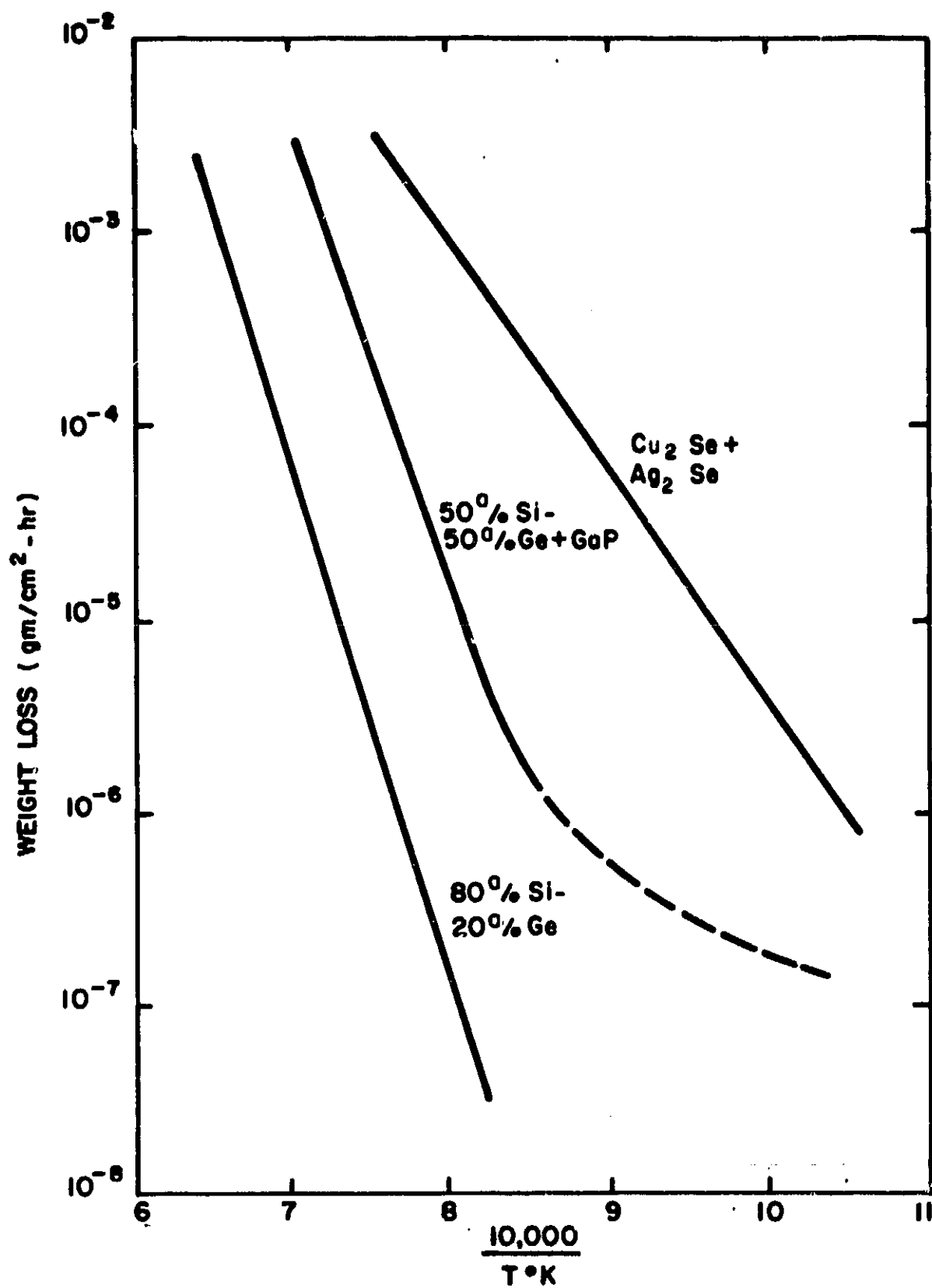


Figure 6. Weight Loss Characteristics of Various Thermoelectric Materials.

### III. LANTHANUM CHROME SULFIDE

The choice of  $\text{LaCrS}_3$  as the material to be investigated on the present program, was partly based on literature data on the material and partly on experimental results of this program.  $\text{LaCrS}_3$  is a semiconductor material with a band gap of about 1.3 electron volts and a melting temperature of  $1650^\circ\text{C}$ . This material possesses very low values of thermal conductivity (in the range of  $10\text{mw}/^\circ\text{C}\text{-cm}$ ) and it can be doped to tailor its electrical properties. All of these characteristics are prerequisites of good thermoelectric materials and it is especially the band gap and melting temperature that make  $\text{LaCrS}_3$  attractive as a thermoelectric material capable of operation to about  $1000^\circ\text{C}$ . The band gap of 1.3 electron volts implies that in an extrinsic state, the material remains so throughout its intended operating temperature range of up to  $1000^\circ\text{C}$ . The melting temperature of  $1650^\circ\text{C}$  implies that at this operating temperature of  $1000^\circ\text{C}$ , the material is at temperatures at which the vapor pressure of the material should be quite low.

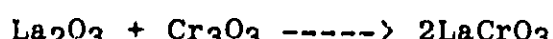
Much of the effort on lanthanum chrome sulfide on the current program has been devoted to efforts to prepare stoichiometric  $\text{LaCrS}_3$ . Initially this effort utilized stoichiometric quantities of lanthanum, chromium, and sulfur in evacuated quartz ampules that were reacted at temperatures in the range of 500 to  $1000^\circ\text{C}$ . Invariably it was found that two phase material resulted. It is believed that the chromium preferentially reacted to form  $\text{Cr}_2\text{S}_3$ . The remaining

lanthanum and sulfur reacted to form  $\text{La}_2\text{S}_3$ . The result was a mixture of these two compounds. More recent efforts have included iodine as a catalyst and it has been found that small quantities of  $\text{LaCrS}_3$  are formed when the reaction is performed in a temperature gradient. Even in this case, however, most of the reaction product is in the form of a mixture of  $\text{La}_2\text{S}_3$  and  $\text{Cr}_2\text{S}_3$ . Extensive experiments have been conducted in which the quantities of iodine and temperature gradient during reaction have been varied in an effort to optimize the yield of  $\text{LaCrS}_3$  in the reaction. Even under optimum conditions, it has been found that the reaction proceeds extremely slowly and that the yield of stoichiometrical  $\text{LaCrS}_3$  is small. A practical consideration in the preparation of  $\text{LaCrS}_3$  by this method is that it is difficult to separate the  $\text{LaCrS}_3$  from the rest of the reacted material.

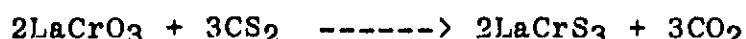
A number of ampules containing lanthanum, sulfur and chromium were reacted in attempts to prepare  $\text{LaCrS}_3$ . In all cases, the bulk of the reaction products were  $\text{La}_2\text{S}_3$  and  $\text{Cr}_2\text{S}_3$ , with a small amount of  $\text{LaCrS}_3$  in the form of single crystal flakes that adhered to the inner surface of each ampule. Although initial attempts to form  $\text{LaCrS}_3$  did not use catalysts, based on literature sources, it was decided in subsequent efforts to include small amounts of iodine in the reaction. It was found that the yeild of  $\text{LaCrS}_3$  was proportional to the quantity of iodine used in the reaction. It was also found that the greatest yield of desired material

resulted when the reaction was performed in a temperature gradient, with one end of each ampule at 1070°C and the other end of the ampule at 940°C.

In view of the difficulties experienced in attempts to prepare  $\text{LaCrS}_3$ , a literature search was undertaken to find other ways in which the material can be prepared. It appears that  $\text{LaCrS}_3$  has been prepared by investigators in both Japan and France. The method used by both groups of investigators involves the reaction of lanthanum oxide and chromium oxide to form lanthanum chrome oxide, as follows:



At the completion of this reaction, the lanthanum chrome oxide is converted to lanthanum chrome sulfide by passing carbon disulfide over the lanthanum chrome oxide, as follows:



According to the literature, in the presence of carbon disulfide, the lanthanum chrome oxide is totally converted to lanthanum chrome sulfide. Moreover, the reaction between the two oxides to form lanthanum chrome oxide supposedly proceeds readily and can be performed quite quickly.

While consideration was given to a new method of preparation of  $\text{LaCrS}_3$ , an evaluation was conducted of the material prepared by reaction of powders in quartz ampules. The material is in the form of flakes that generally adhere to the inner surfaces of the quartz ampules; the remainder of the material, a mixture of  $\text{La}_2\text{S}_3$  and  $\text{Cr}_2\text{S}_3$ , occurs within the volumes of the ampules. The  $\text{LaCrS}_3$  flakes are carefully

removed from the inner surfaces of the ampules with stainless steel tweezers and stored in stoppered glass jars. Inasmuch as the yield of  $\text{LaCrS}_3$  is low, only a few hundred milligrams of the material is obtained from each reacted ampule. All of the material prepared in eight separate ampules was combined and weighed to assess the availability of sufficient material for hot pressing into a sample. It was found that a total of about 1.54 grams of the  $\text{LaCrS}_3$  flakes exist. When these flakes are hot pressed into a 0.25 inch diameter pellet, it was calculated from the known density of  $\text{LaCrS}_3$  that the pellet would have a length of about 0.4 inch. Although a pellet of these dimensions is quite small, it is nevertheless of adequate size for the measurement of its electrical characteristics. For this reason it was decided to hot press the available  $\text{LaCrS}_3$  flakes into a pellet.

Although x-ray diffraction measurements of the flakes have confirmed that the material is essentially  $\text{LaCrS}_3$ , it has been observed that the material also exhibits some very low intensity x-ray peaks that are not characteristic of  $\text{LaCrS}_3$  and, in fact, appear to correspond to x-ray peaks associated with  $\text{La}_2\text{S}_3$ . The possibility thus exists that the flakes of  $\text{LaCrS}_3$  contain a small fraction of an  $\text{La}_2\text{S}_3$  component either in the bulk or as a surface contaminant. Surface contamination of the flakes is possible because, as mentioned above, the reaction that produces  $\text{LaCrS}_3$  also produces  $\text{La}_2\text{S}_3$  and  $\text{Cr}_2\text{S}_3$ . However, x-ray diffraction measurements have not shown the existence of iodine, oxygen,



lanthanum and chromium metals or oxides and chrome sulfide within the  $\text{LaCrS}_3$  flakes. The absence of chrome sulfide reduces the likelihood of surface contamination of the flakes because it might be anticipated that if the flakes are contaminated with one of the two sulfides, they should be contaminated with both; both compounds exist in the environment of the reacted  $\text{LaCrS}_3$ . It is thus tentatively concluded that the  $\text{La}_2\text{S}_3$  detected within  $\text{LaCrS}_3$  flakes is within the bulk of the material. What effect the presence of  $\text{La}_2\text{S}_3$  within  $\text{LaCrS}_3$  has on the properties of the material is not known. The concentration of the  $\text{La}_2\text{S}_3$  component, however, is very small because the  $\text{LaCrS}_3$  flakes consist of a single phase. It may be expected that a large concentration of  $\text{La}_2\text{S}_3$  within the  $\text{LaCrS}_3$  matrix would result in a two phase system because the crystal structures of the two materials are different.

An existing hot pressing die was prepared with a graphite sleeve of the required 0.25 inch inner diameter. The material in the form of small flakes of  $\text{LaCrS}_3$  was loaded into the die and the die was placed into the hot press and evacuated. The die was outgassed at  $500^\circ\text{C}$  for several hours before being heated to the pressing temperature of  $1200^\circ\text{C}$ . Once at  $1200^\circ\text{C}$ , a pressure of 35,000 psi was applied and maintained for two hours. The sample was cooled from its pressing temperature of  $1200^\circ\text{C}$  to  $400^\circ\text{C}$  over the period of one hour. Another hour was expended in cooling the sample from  $400^\circ\text{C}$  to room temperature. At the completion of pressing, the pressure on the sample was

allowed to decrease slowly while the sample cooled. By the time the sample had cooled to room temperature, pressure had decreased to zero.

The sample was extracted from the die by a special core drill that cut through the graphite sleeve; this procedure eliminates the necessity to apply pressure to the sample to extract it from the die. After removal from the die, the graphite layers adhering to the sides and ends of the sample were removed by lapping. The final size of the sample was determined to be 0.6 cm diameter and 0.8 cm height. A visual microscopic examination of the sample did not reveal any cracks. A density determination yielded the value of 4.6 grams per cubic centimeter for the sample. This value is consistent with the literature value of 4.5 grams per cubic centimeter for the density of  $\text{LaCrS}_3$ .

Prior to the measurement of the electrical characteristics of the sample of  $\text{LaCrS}_3$ , a new property measurement apparatus was designed and constructed. With this apparatus it is possible to obtain measurement to  $1200^\circ\text{C}$ , rather than the  $700^\circ\text{C}$  previously possible. The new measurement apparatus is schematically shown in Figure 7. The apparatus makes use of a furnace as the sample closure. A heater placed at one end of the sample enables the imposition of a temperature gradient across the sample for Seebeck coefficient measurements. A weight external to the heater loads the sample to molybdenum electrodes at its ends; these electrodes are used for the passing of current through the sample in the performance of

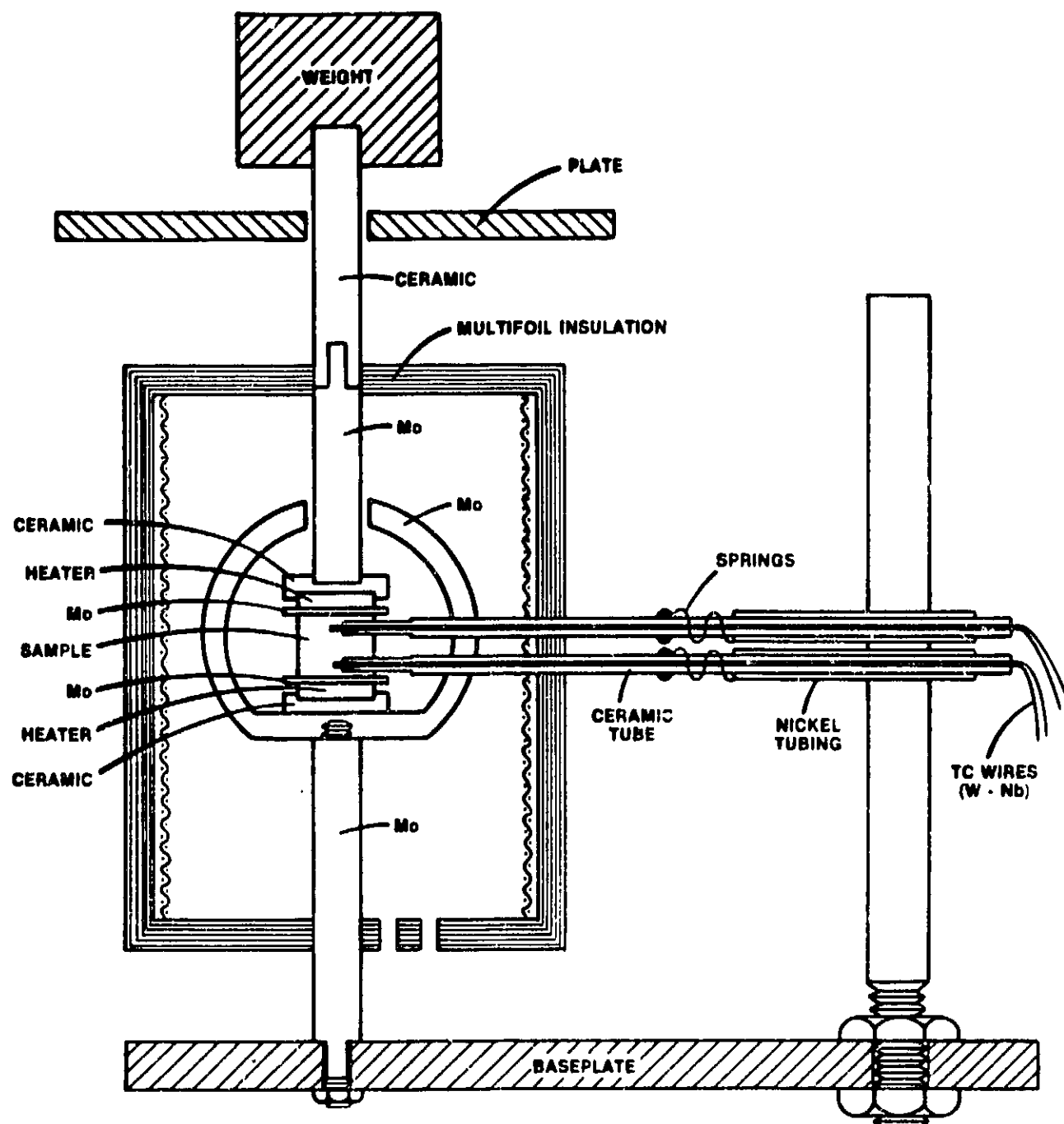


Figure 7. High Temperature Thermoelectric Property Measurement Apparatus.

electrical resistivity measurements. The significant feature of the apparatus is the spring-loading of two thermocouple contained in alumina tubes into holes drilled in the side of the sample. This assures continuous contact between the thermocouple beads and the sample and also guarantees that only the beads of the thermocouple touch the sample - hence the Seebeck voltage and temperatures are measured at identical locations. Because the apparatus makes use of high temperature molybdenum heater wires and the heater is shielded by multifoil insulation, the thermoelectric properties of test samples measured in the apparatus can be determined at temperatures up to about 1200 to 1300°C.

The results of the electrical property measurements on the sample of  $\text{LaCrS}_3$  hot pressed from single crystal flakes are shown in Figures 8 to 10. Figure 8 shows a plot of electrical resistivity as a function of temperature for six separate measurement cycles on different dates. Following the sequence of dates, it is apparent in Figure 8 that the electrical resistivity of the sample decreases with annealing; this is even seen during individual measurement cycles, e.g. those during 24 March and 29 March 1983. The sample was maintained at 1125°C during the night of 29/30 March and, as seen in Figure 8, its resistivity decreased from about 33 milliohm-centimeters to 20 milliohm-centimeters.

The corresponding data for the Seebeck coefficient are shown in Figure 9. It is noted in Figure 9 that the Seebeck coefficient of the sample decreased with annealing in a manner

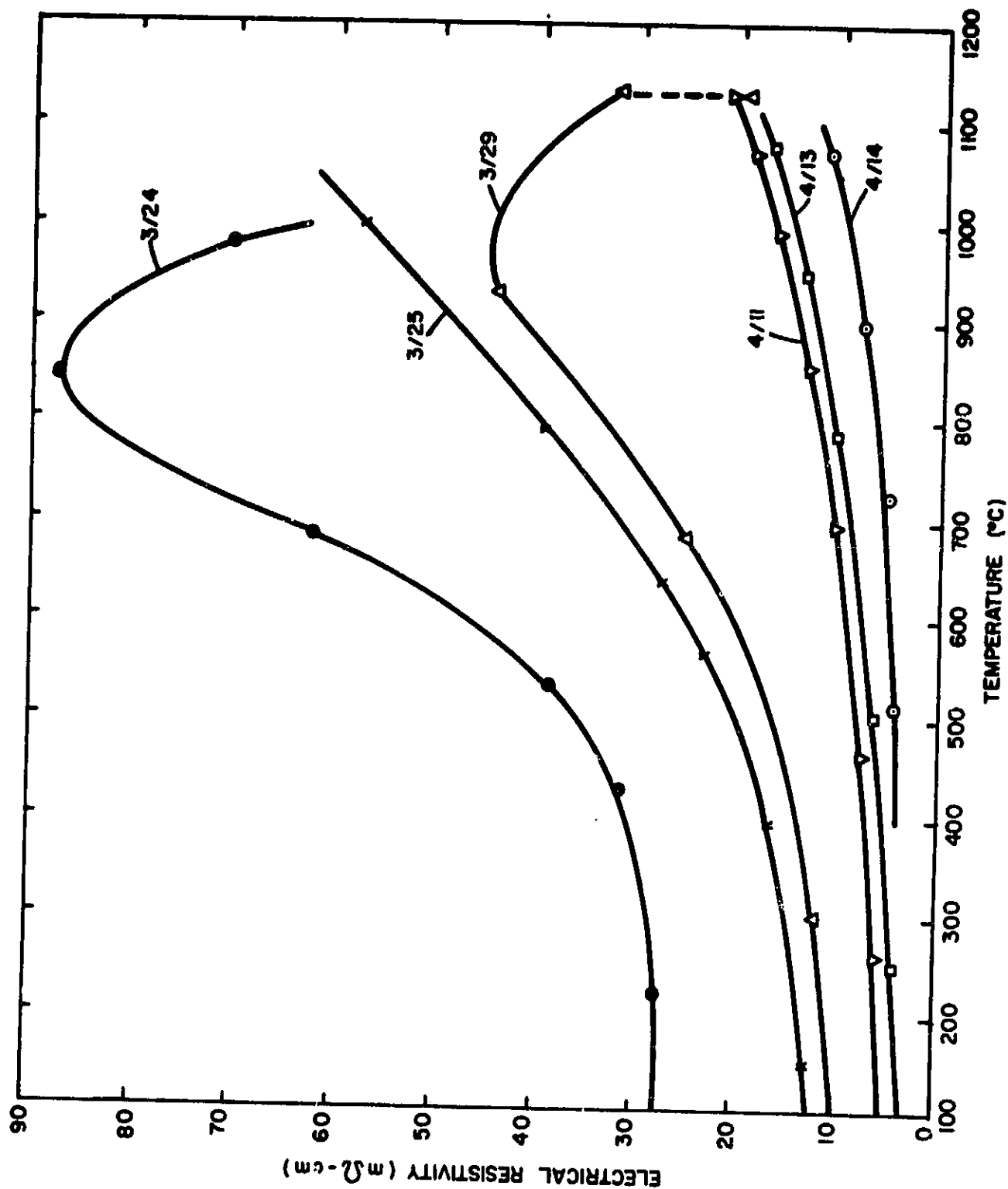


Figure 8. Electrical Resistivity of  $\text{LaCrS}_3$  as a Function of Annealing.

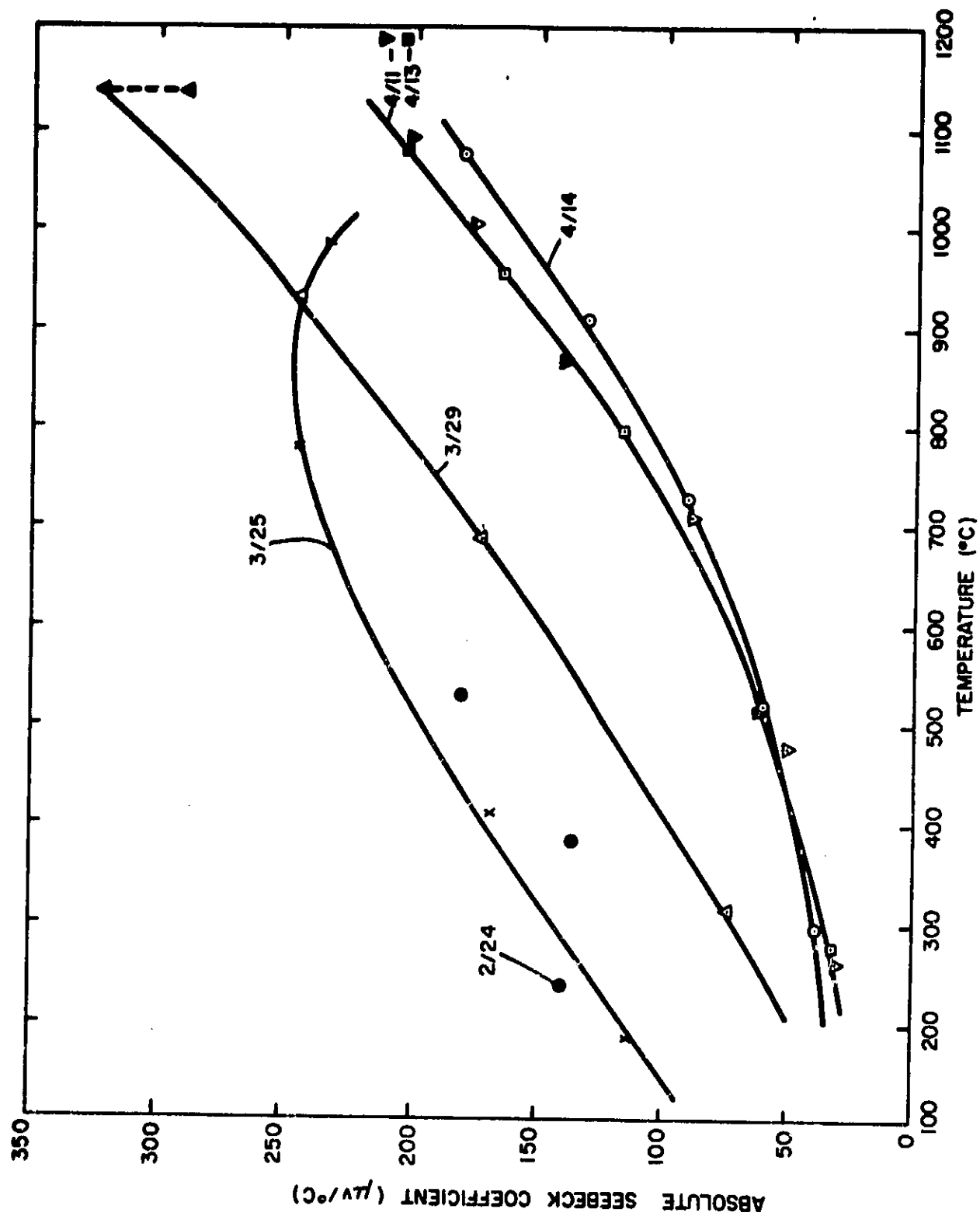


Figure 9. Absolute Seebeck Coefficient of  $\text{LaCrS}_3$  as a Function of Annealing.

analogous to that of the electrical resistivity. Inasmuch as both properties decreased with annealing, it is concluded that the reason for it is an increasing carrier concentration with time.

Although the individual thermoelectric properties of the material may change with time, this does not reflect the worth of the material unless the properties are combined in a form that is proportional to the performance of the material. Such a combination of the properties is the quotient of the square of the Seebeck coefficient and the electrical resistivity. When the property data in Figures 8 and 9 are combined in this manner, the results are the "power factors" of the material at different times. These "power factors" are plotted in Figure 10 as a function of temperature for the data obtained on the sample of  $\text{LaCrS}_3$  during the last three measurement cycles. It is noted in Figure 10 that the "power factor" not only increases with temperature, but also increases with annealing. If it is assumed that the thermal conductivity of  $\text{LaCrS}_3$  is of the order of 0.005 to 0.010 milliwatts/ $^{\circ}\text{C}$ -centimeter, it is concluded that at the highest temperature shown in Figures 8 to 10, the figure-of-merit of the material is of the order of the same magnitude as that of silicon-germanium alloys. Inasmuch as the "power factor" is still increasing with annealing, it is not known how high it may ultimately rise. In any case,  $\text{LaCrS}_3$  shows great promise as a good thermoelectric material. After the last measurement cycle of 14 April 1983, the sample was sent to JPL for independent measurements.

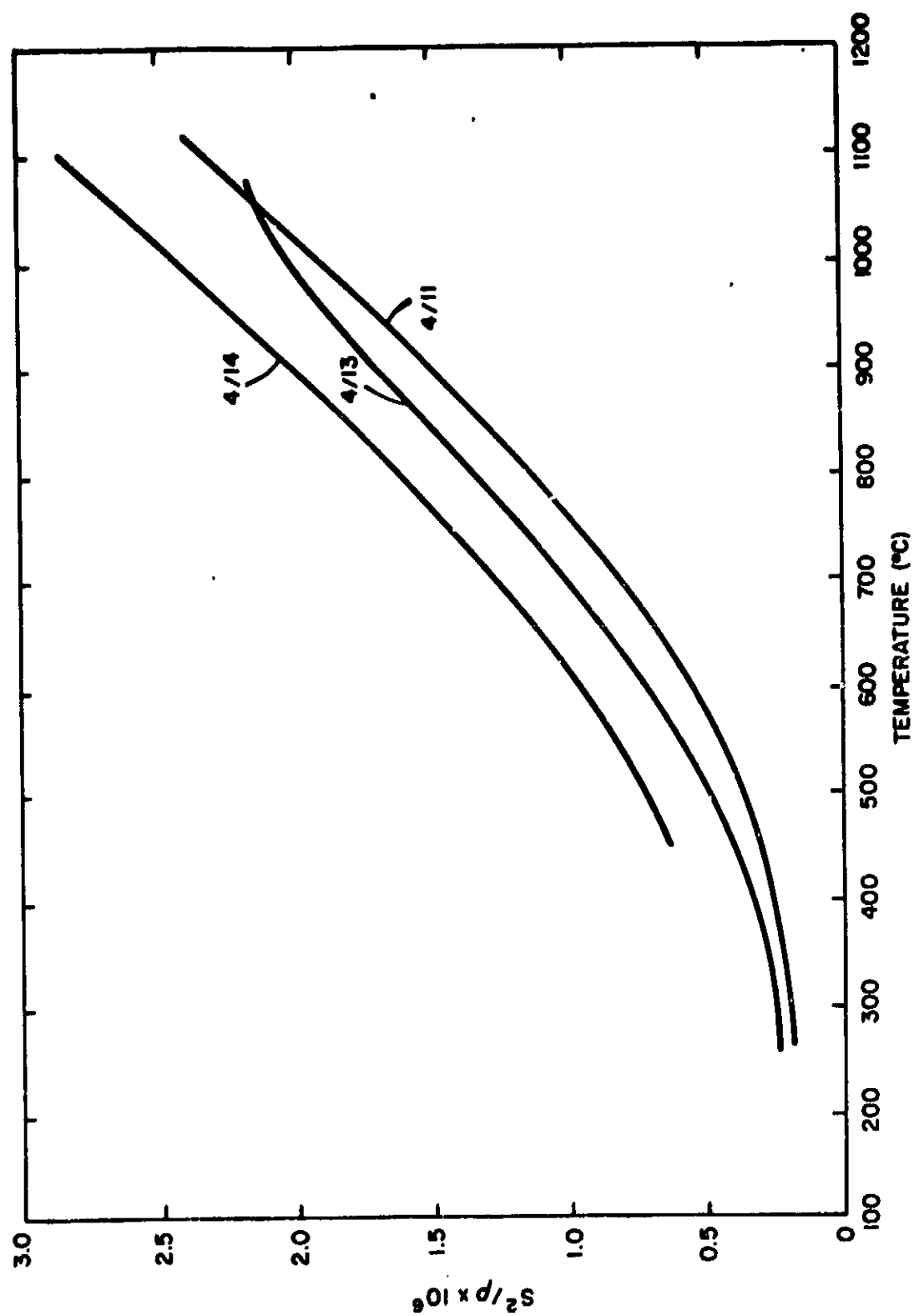


Figure 10. Power Factor of  $\text{LaCrS}_3$  as a Function of Annealing.



#### IV. CHROME SULFIDE AND LANTHANUM SULFIDE

As discussed above, attempts to synthesize lanthanum chrome sulfide on the present program have resulted in only small quantities of the desired material, with the bulk of the reacted material in the form of a mixture of lanthanum sulfide ( $\text{La}_2\text{S}_3$ ) and chrome sulfide ( $\text{Cr}_2\text{S}_3$ ). Inasmuch as both of these materials are semiconductors that reportedly exhibit reasonable thermoelectric characteristics, it was decided on the present program to investigate their mixtures in various proportions. It is generally known that the alloying of two materials results in a material that possesses better thermoelectric characteristics than either of the constituents because alloying results in significantly reduced values of thermal conductivity.

A number of alloys of  $\text{La}_2\text{S}_3$  and  $\text{LaCr}_3$  have been hot pressed and characterized. The characterization has involved the material in its as-prepared state, as well as after various periods of high temperature annealing. Although not optimized, it has been found that alloys of  $\text{La}_2\text{S}_3$  and  $\text{Cr}_2\text{S}_3$  offer considerable promise as good thermoelectric materials.

Samples of alloys of  $\text{La}_2\text{S}_3$  and  $\text{Cr}_2\text{S}_3$  have been hot pressed and characterized in the comparative thermal conductivity apparatus. These alloys can be generally expressed as  $(\text{La}_2\text{S}_3)_{1-x}(\text{Cr}_2\text{S}_3)_x$ . The results on these alloys can be summarized by three compositions having values of  $x$  of 0.25, 0.48 and 0.65. Aside from the composition difference, there was a difference in the lanthanum metal of

these alloys. The sample with x of 0.25 was made with high purity lanthanum from Ames Laboratory whereas the other two samples were made with lanthanum obtained from Alfa Ventron. The latter lanthanum contains oxygen as an impurity. After hot pressing and before detailed property measurements, each of the three alloy samples was annealed in vacuum for a period of time of about 150 hours at 1000°C.

The thermal conductivity values of the three samples are shown in Figure 11 as a function of temperature. It is noted that the sample with the composition  $(\text{La}_2\text{S}_3)_{0.75}(\text{Cr}_2\text{S}_3)_{0.25}$  has a thermal conductivity that is appreciably lower than the thermal conductivities of the other two samples. As will be seen below, the differences in the thermal conductivities are primarily due to the electronic part of the total thermal conductivity. The electrical resistivity values of the sample with the composition  $(\text{La}_2\text{S}_3)_{0.75}(\text{Cr}_2\text{S}_3)_{0.25}$  are much higher than those of the other two samples. The respective values of electrical resistivity of the three samples are plotted as a function of temperature in Figures 12 and 13. Finally the Seebeck coefficient values of all three samples are plotted as a function of temperature in Figure 14. It is noted in Figure 14 that all three samples have Seebeck coefficient values quite similar to each other.

As mentioned above, prior to the performance of property measurements, the three samples depicted by data in Figures 11 to 14 were annealed for 150 hours at 1000°C. Whereas the

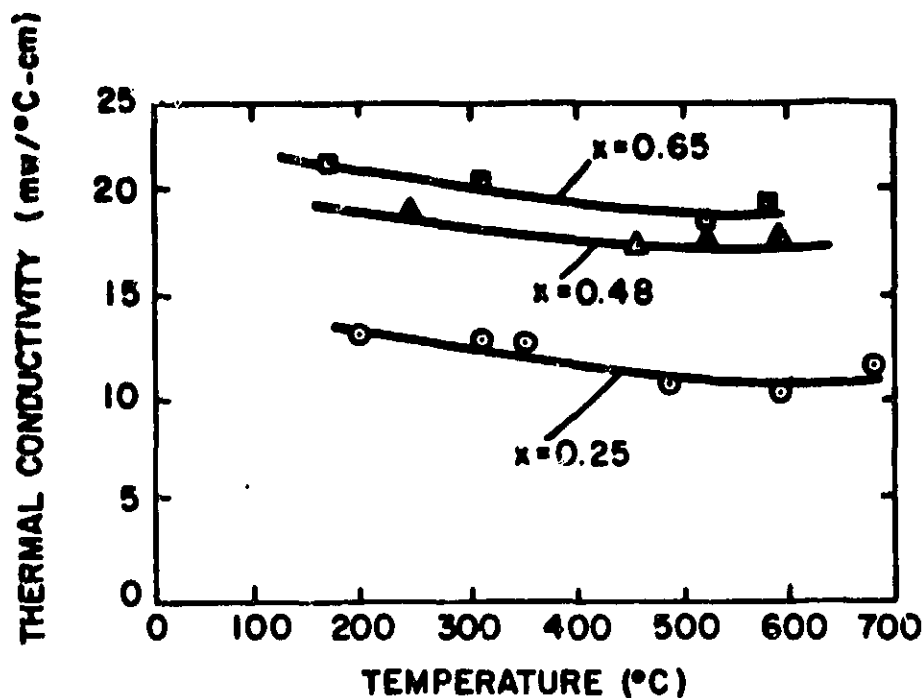


Figure 11. Temperature Dependence of the Thermal Conductivity of  $(\text{La}_2\text{S}_3)_{1-x}(\text{Cr}_2\text{S}_3)_x$  Solid Solutions.

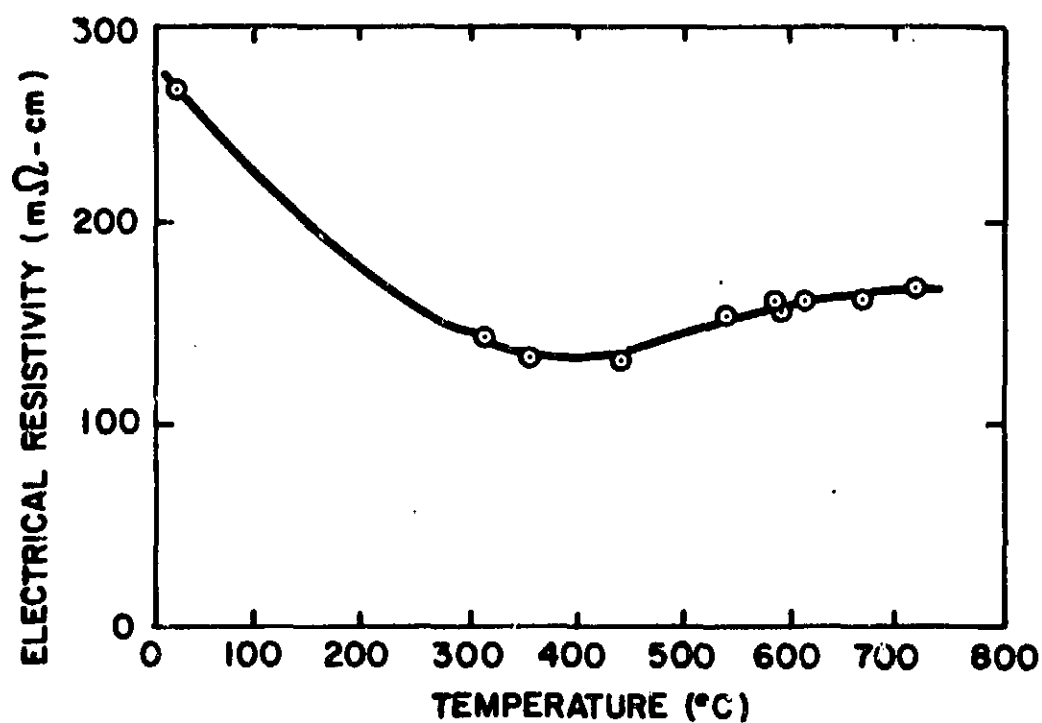


Figure 12. Temperature Dependence of the Electrical Resistivity of  $(\text{La}_2\text{S}_3)_{0.75}(\text{Cr}_2\text{S}_3)_{0.25}$ .

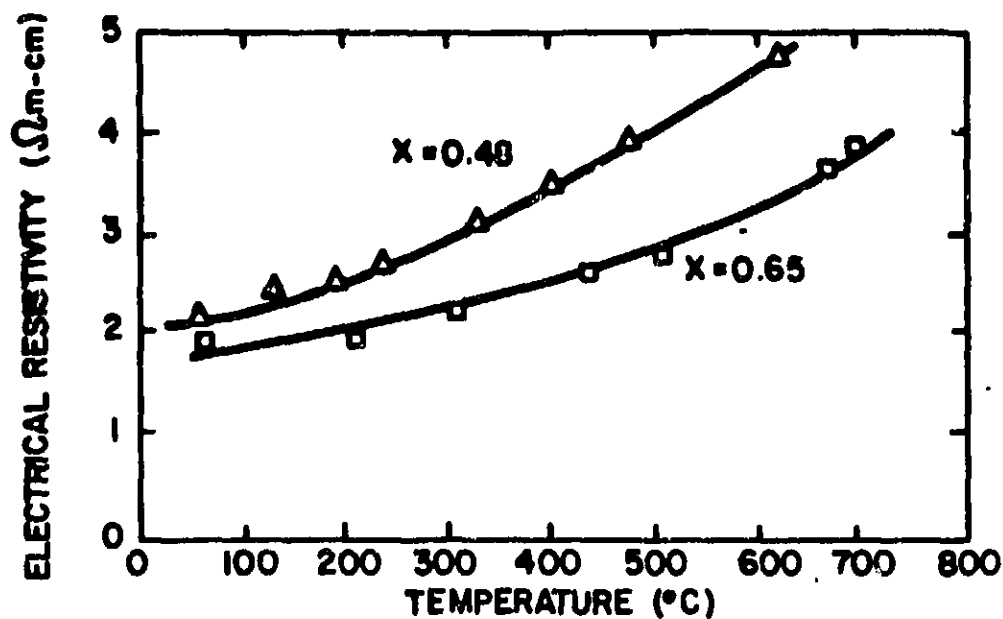


Figure 13. Temperature Dependence of the Electrical Resistivity of  $(\text{La}_2\text{S}_3)_{1-x}(\text{Cr}_2\text{S}_3)_x$  Solid Solutions.

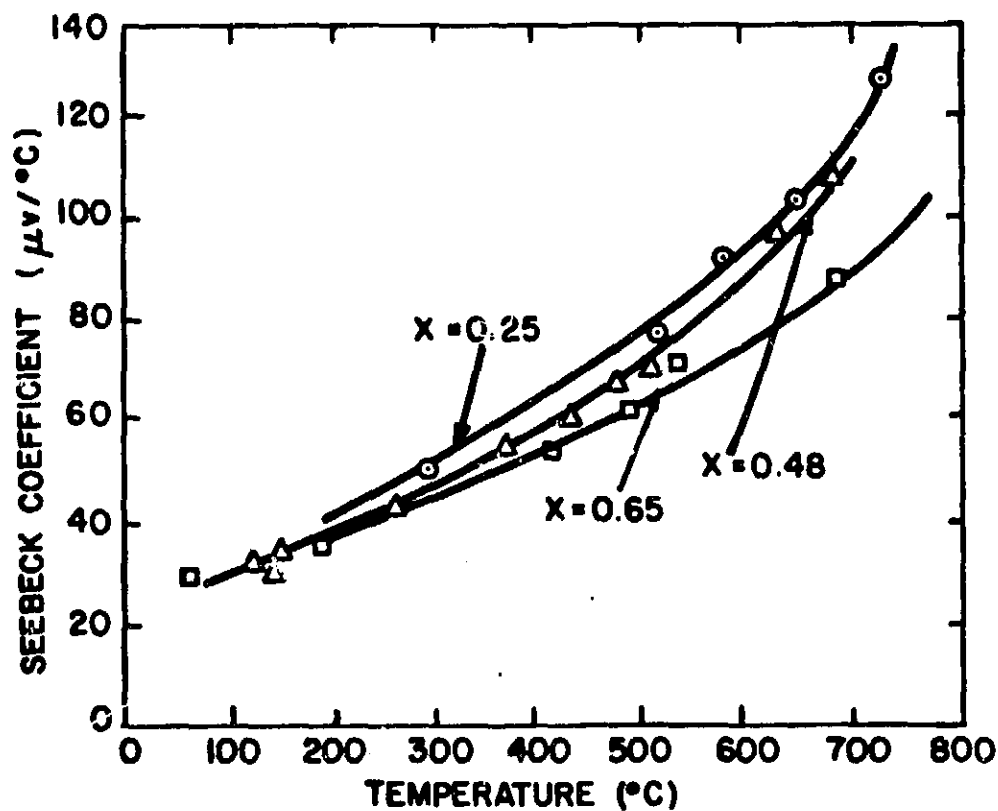


Figure 14. Seebeck Coefficient of  $(\text{La}_2\text{S}_3)_{1-x}(\text{Cr}_2\text{S}_3)_x$  Solid Solutions.

electrical resistivities of all samples decreased appreciably during annealing, the Seebeck coefficient and thermal conductivity values were little affected by the annealing procedure. This implies that annealing of the material results in decreased values of carrier mobility, with little change in the carrier concentration. An explanation for this phenomenon is the homogenization of the material during annealing that results in decreased carrier scattering at grain boundaries within the material.

In view of the foregoing, it may be anticipated that annealing of alloys of  $\text{La}_2\text{S}_3$  and  $\text{Cr}_2\text{S}_3$  results in increasing values of figure-of-merit. This, in fact, is the case and is illustrated in Figure 15 for the  $(\text{La}_2\text{S}_3)_{0.75}(\text{Cr}_2\text{S}_3)_{0.25}$  sample. It is noted in Figure 15 that annealing of the material at  $1000^\circ\text{C}$  for 150 hours has resulted in nearly two order of magnitude increase in figure-of-merit; the increase in figure-of-merit is directly proportional to a decrease in electrical resistivity because the Seebeck coefficient and thermal conductivity are unchanged from the values shown in Figures 11 and 14.

Finally, the figure-of-merit values of all three test samples depicted by the data in Figures 11 to 14 are shown as a function of temperature in Figure 16. It is noted in Figure 16 that the two samples with greater  $\text{Cr}_2\text{S}_3$  contents possess higher values of figure-of-merit than does the sample that is richer in  $\text{La}_2\text{S}_3$ . It is not known whether this finding is significant or only reflects the degree of relative annealing of the three test samples.

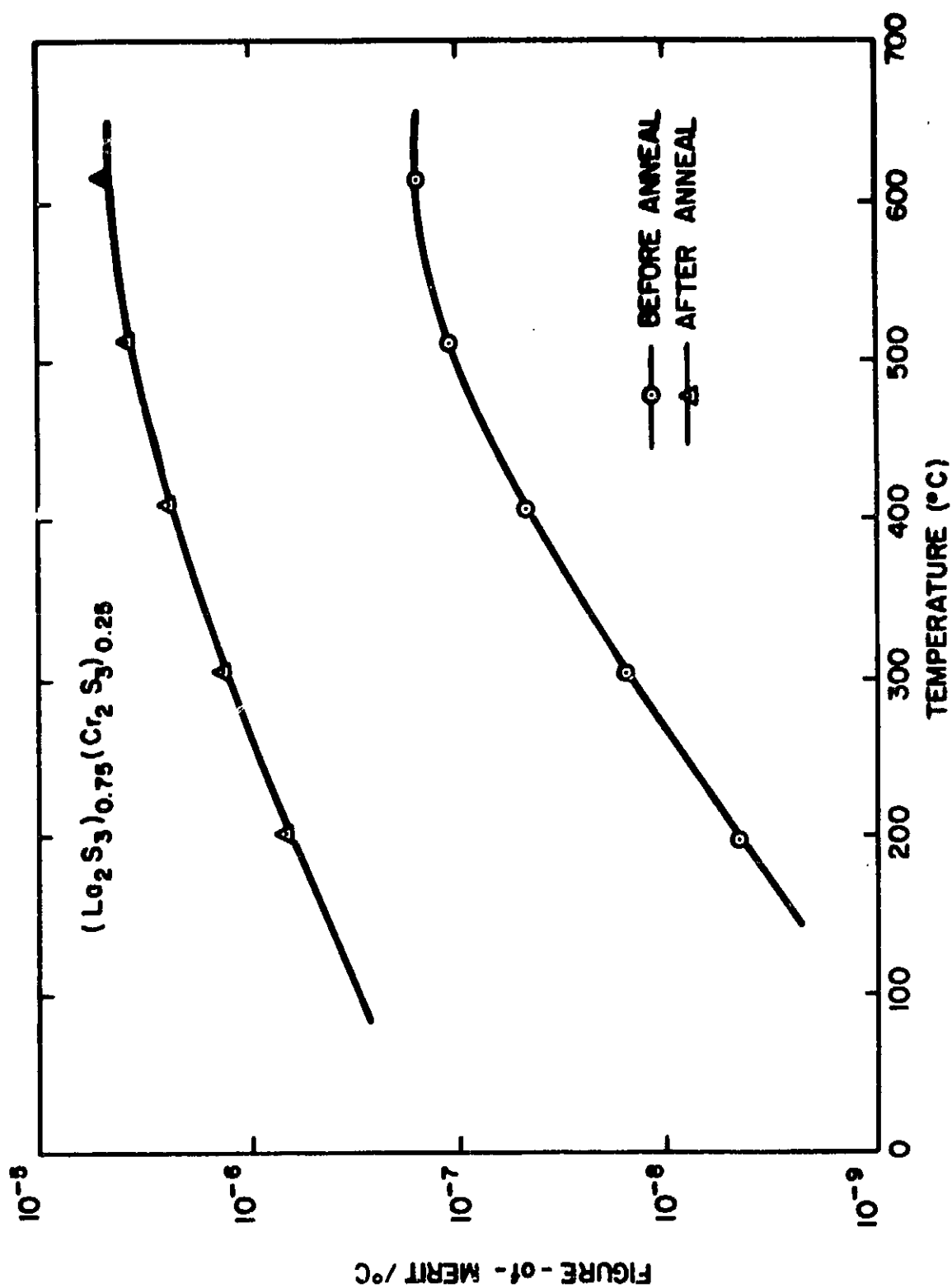


Figure 15. Figure-of-Merit of  $(La_{0.25}S_3)_{0.75}(Cr_2S_3)_{0.25}$  as a Function of Annealing.

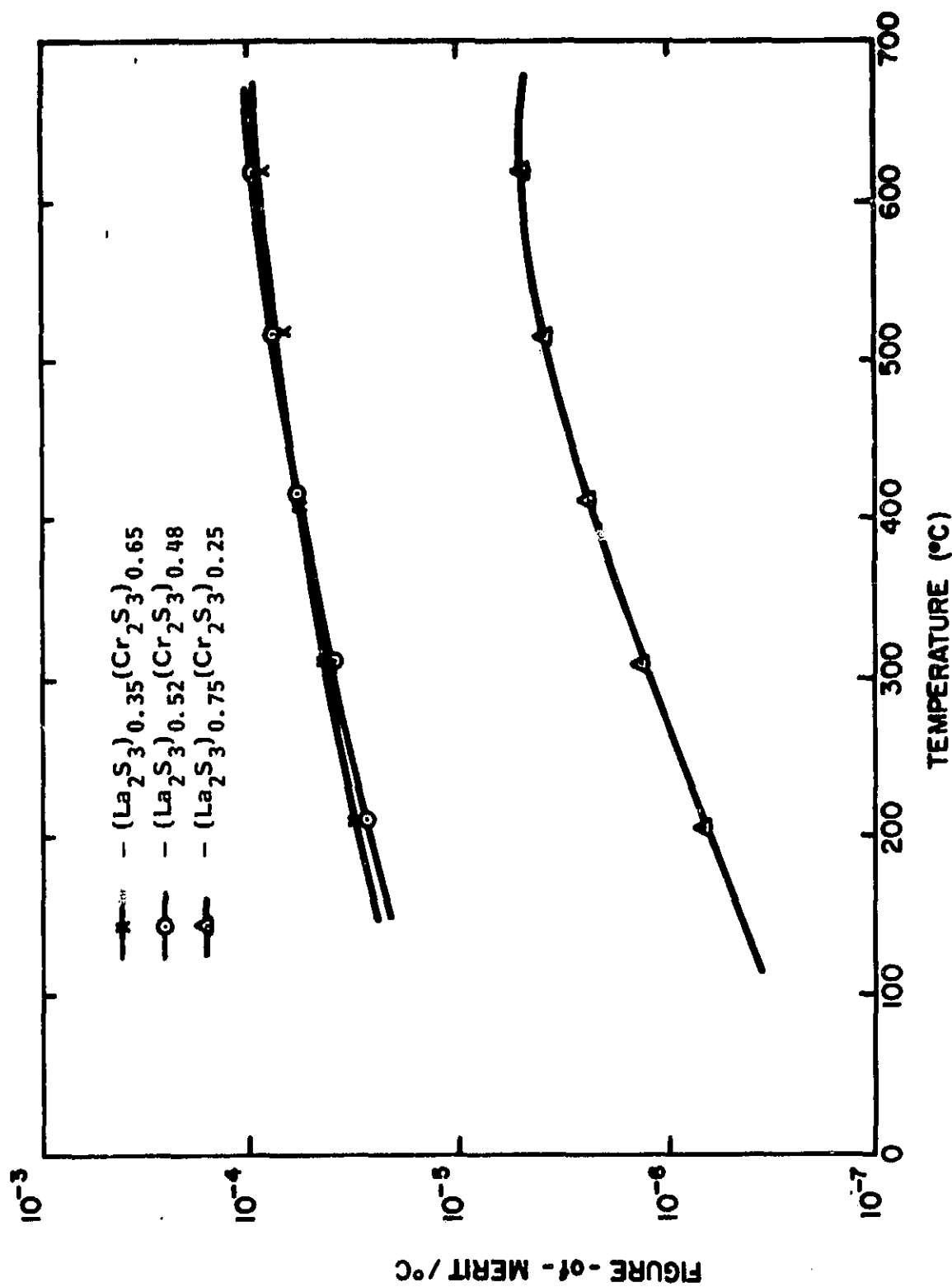


Figure 16. Figures-of-Merit of Various Mixtures of  $\text{La}_2\text{S}_3$  and  $\text{Cr}_2\text{S}_3$  After Annealing.

The sample of  $(\text{La}_2\text{S}_3)_{0.75}$   
 $(\text{Cr}_2\text{S}_3)_{0.25}$  originally measured in the comparative  
thermal conductivity apparatus (see Figures 11, 12, 14) was  
remeasured in the high temperature apparatus that was discussed  
in Section III. The results of the measurements are shown in  
Figures 17 and 18 in terms of plots of electrical resistivity  
and Seebeck coefficient as functions of temperature. It is  
noted in Figures 17 and 18 that generally good agreement exists  
in the data obtained in the two different measurement  
apparatuses. The agreement in the Seebeck coefficient data is  
remarkable because the data obtained with the new apparatus  
represent a measurement technique in which three different  
voltage values are determined for three different temperature  
gradients at a given average sample temperature; the Seebeck  
coefficient data obtained with the comparative thermal  
conductivity apparatus represent voltage determination for a  
single temperature gradient at any given average sample  
temperature. The thermal conductivity of the sample depicted  
by the data in Figures 17 and 18 is shown in Figure 11. As  
seen in Figure 11, the thermal conductivity of the material  
lies within the stated conductivity range of 10 to 20  $\text{mw}/^\circ\text{C}\text{-cm}$ ,  
although at the lower end of the range.

The thermoelectric property data obtained on samples  
consisting of mixtures of  $\text{La}_2\text{S}_3$  and  $\text{Cr}_2\text{S}_3$  of various  
compositions were analyzed in an effort to determine the  
composition corresponding to the minimum thermal conductivity.  
Inasmuch as each sample considered in the analysis exhibited



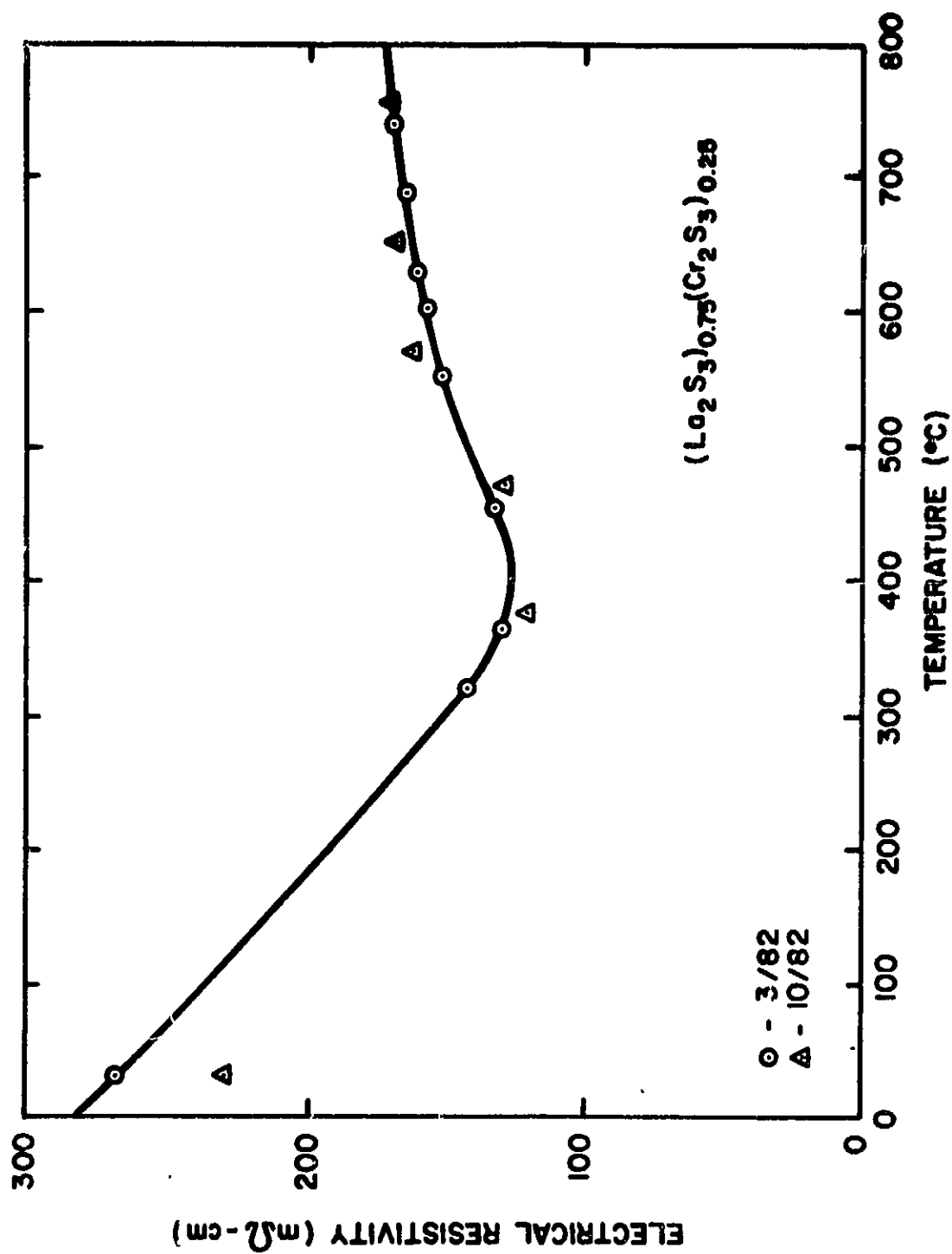


Figure 17. Electrical Resistivity of  $(La_{0.25}S_3)_{0.75}(Cr_2S_3)_{0.25}$ .

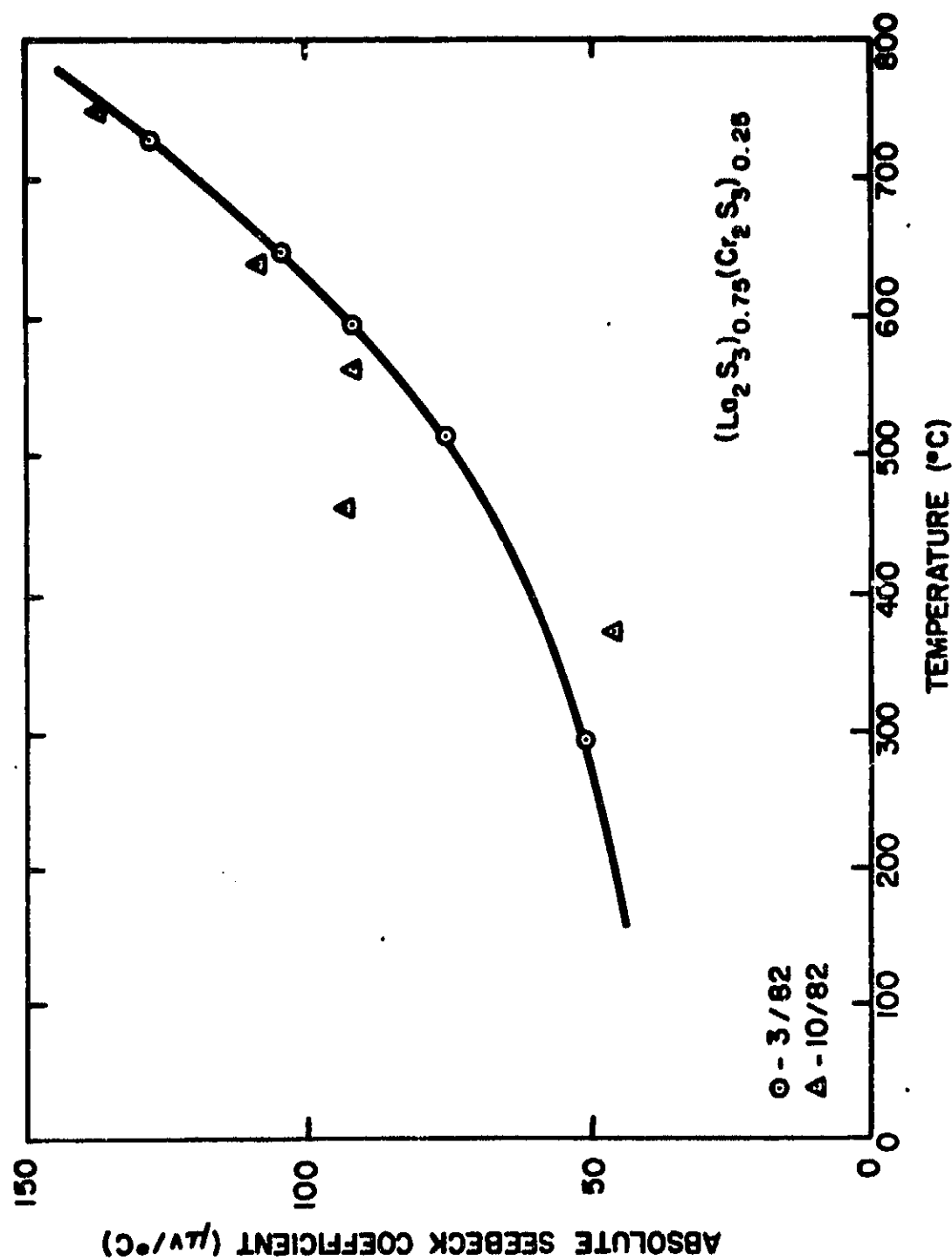


Figure 18. Absolute Seebeck Coefficient of  $(\text{La}_2\text{S}_3)_{0.75}(\text{Cr}_2\text{S}_3)_{0.25}$ .

different values of electrical properties, it was decided to perform the analysis in terms of the lattice component of thermal conductivity in order that the results be consistent. Although none of the samples considered in the analysis had been intentionally doped, a number of them possessed very low values of electrical resistivity and Seebeck coefficient, thereby indicating a high level of carrier concentration. In view of this, it was decided to assume that scattering of carriers in the various samples takes place by impurities. Impurity scattering is associated with Lorenz number,  $L$ , given by  $L = 4(k/e)^2$ , which has a numerical value of  $2.96 \times 10^{-8} \text{ volt}^2/\text{°C}^2$ . The Wiedemann-Franz relationship of  $K_e = L \cdot \sigma \cdot T$ , where  $\sigma$  is electrical conductivity and  $T$  is absolute temperature, was used to calculate the electronic thermal conductivity,  $k_e$ , of the samples being investigated. Subtraction of the electronic thermal conductivity from the total thermal conductivity yielded the lattice thermal conductivity of each sample. The results of the analysis are shown in Figure 19 in terms of the lattice thermal conductivity as a function of temperature for  $\text{La}_2\text{S}_3$  and three different mixtures of  $\text{La}_2\text{S}_3$  and  $\text{Cr}_2\text{S}_3$ . Although the total thermal conductivities of the four samples differed considerably, it is remarkable how similar their lattice thermal conductivities are. The lattice thermal conductivity of  $\text{La}_2\text{S}_3$  appears to be slightly lower than of the other samples, but the difference is within experimental uncertainty and thus is not significant.

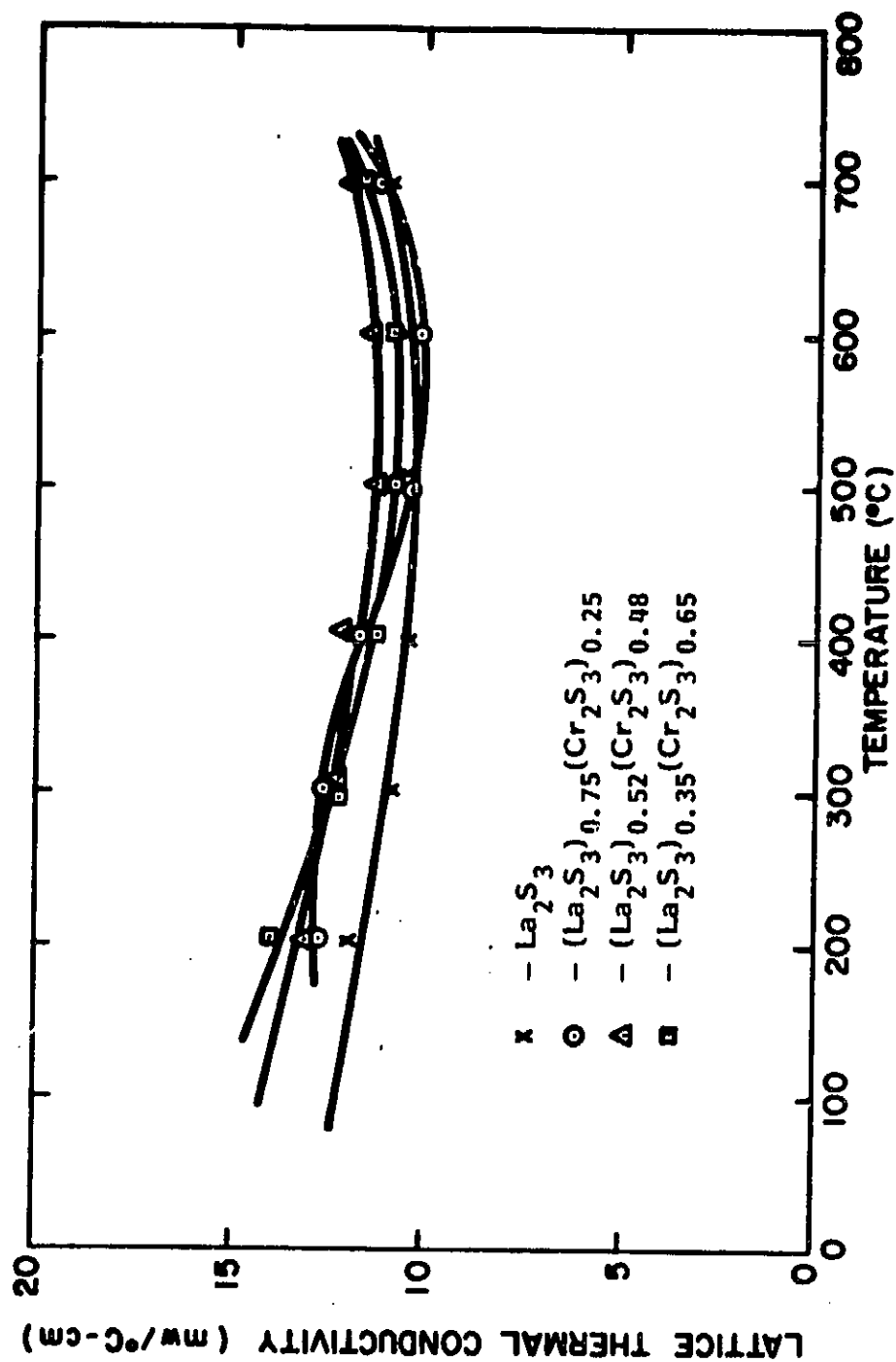


Figure 19. Lattice Thermal Conductivities of Various Mixtures of  $\text{La}_2\text{S}_3$  and  $\text{Cr}_2\text{S}_3$ .

Several conclusions are possible from the data in Figure 19. First, the thermal conductivity of the  $\text{La}_2\text{S}_3$  and  $\text{Cr}_2\text{S}_3$  prepared on the Program are not single phase alloys, but rather two phase mixtures of the constituents. Second, because the compound  $\text{LaCrS}_3$  in essence can be considered a single phase alloy of equal molar proportions of  $\text{La}_2\text{S}_3$  and  $\text{Cr}_2\text{S}_3$ , it may be assumed that its thermal conductivity will be appreciably lower than that of a corresponding mixture of  $\text{La}_2\text{S}_3$  and  $\text{Cr}_2\text{S}_3$ . Third, mixtures of  $\text{La}_2\text{S}_3$  and  $\text{Cr}_2\text{S}_3$  can be optimized solely on the basis of the electrical properties and not the thermal conductivity.

The electrical property data obtained for the sample of  $(\text{La}_2\text{S}_3)_{0.75}(\text{Cr}_2\text{S}_3)_{0.25}$  (see Figures 17 and 18) were analyzed for carrier concentration and mobility in order to obtain a better understanding of the transport properties of alloys of  $\text{La}_2\text{S}_3$  and  $\text{Cr}_2\text{S}_3$ . The analysis consisted of the calculation of carrier concentration and mobility of the sample as a function of temperature. The carrier concentration of the sample was calculated by means of the following relationship for the Seebeck coefficient,

$$S = \frac{k}{e} \left[ 2 + \ln \frac{N_c}{n} \right]$$

where  $k$  is the Boltzmann constant,  $e$  is the electronic charge,  $n$  is carrier concentration and  $N_c$ , the density of states, is given by

$$N_c = 2.35 \times 10^{-15} (\text{mT})^{3/2}$$

with  $m$  the effective carrier mass and  $T$  absolute temperature. The numerical factor of 2 in the Seebeck coefficient expression assumes that carrier scattering is of the acoustic mode. The carrier concentration calculated from actual measured Seebeck coefficient data are plotted as a function of temperature in Figure 20 on the basis of an assumed value of 2.5 for carrier effective mass. This value for carrier effective mass is one reported for  $\text{La}_2\text{S}_3$  in the literature. It is noted in Figure 20 that carrier concentration increases with temperature, although the rate of increase decreases with increasing temperature. At the highest temperatures of 700 to 800°C, the carrier concentration is constant. This implies that the carriers are excited from an impurity level in the band gap. The energy of the impurity level is such that at 700°C all the impurities have been ionized.

The carrier mobility,  $\mu$ , is calculated from the electrical resistivity,  $\rho$ , as follows:

$$\rho = \frac{1}{ne\mu}$$

The calculated mobility of the material as a function of temperature is shown in Figure 21. Superimposed on Figure 21 is a plot with the temperature dependence of  $T^{-3/2}$ . It is noted that the actual data possess the  $T^{-3/2}$  temperature dependence at temperatures higher than 300°C. Inasmuch as acoustic mode scattering possesses the

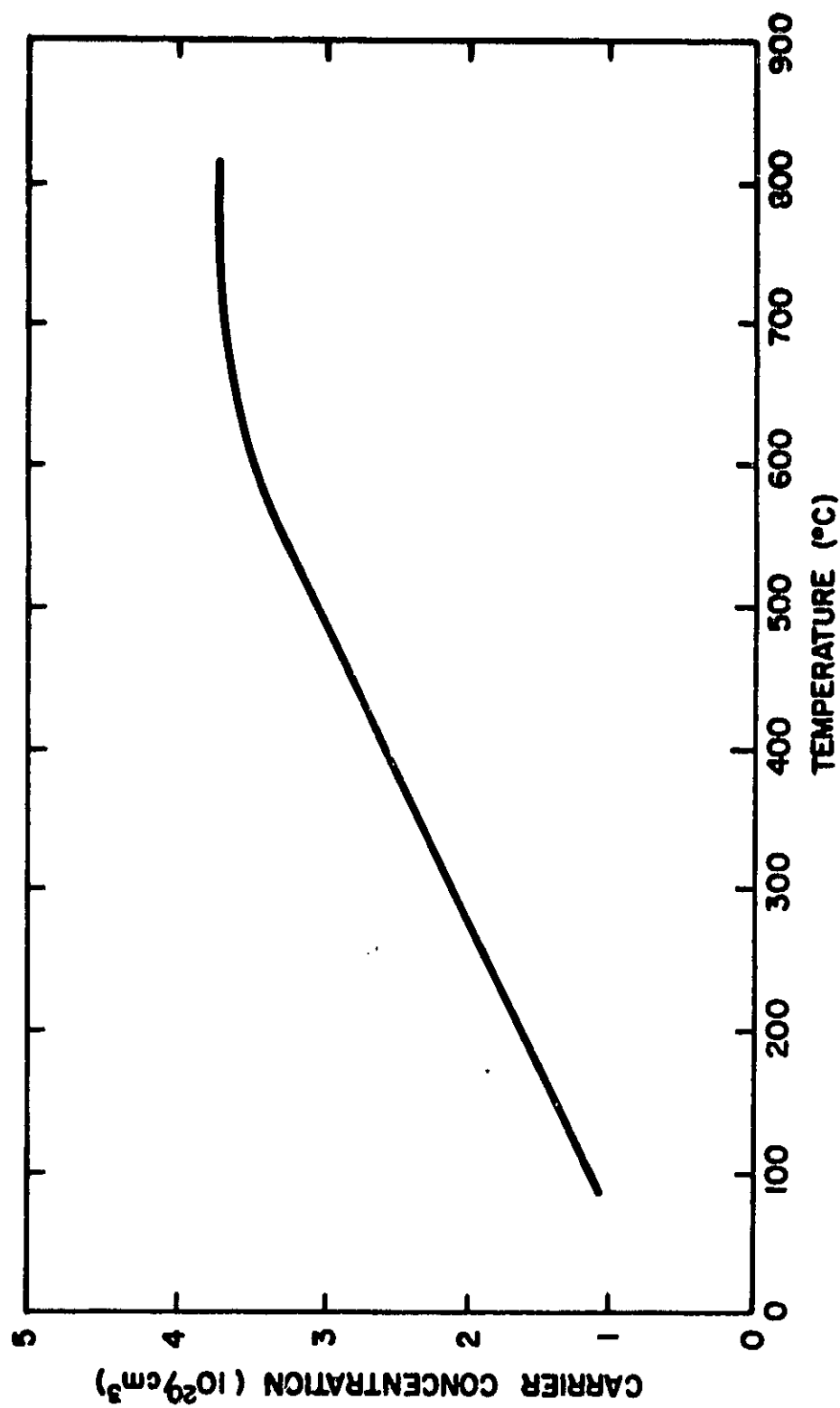


Figure 20. Carrier Concentration of  $(\text{La}_2\text{S}_3)_{0.75}(\text{Cr}_2\text{S}_3)_{0.25}$ .

$T^{-3/2}$  temperature dependence, it is felt that the assumption of this scattering mechanism in connection with the calculation of carrier concentration is justified.

It should be noted that the above analysis uses equations applicable to non-degenerate materials; the carrier concentration values of above  $10^{20}$  per cubic centimeter indicate that the material is partly degenerate and for this reason the results are only approximate. The assumed effective mass of 2.5 may be too high because  $\text{La}_2\text{S}_3$  has a band gap considerably higher than that of  $\text{LaCrS}_3$ . If a lower value of effective mass is used in the analysis, the calculated values of carrier concentration will decrease and carrier mobility values will increase.



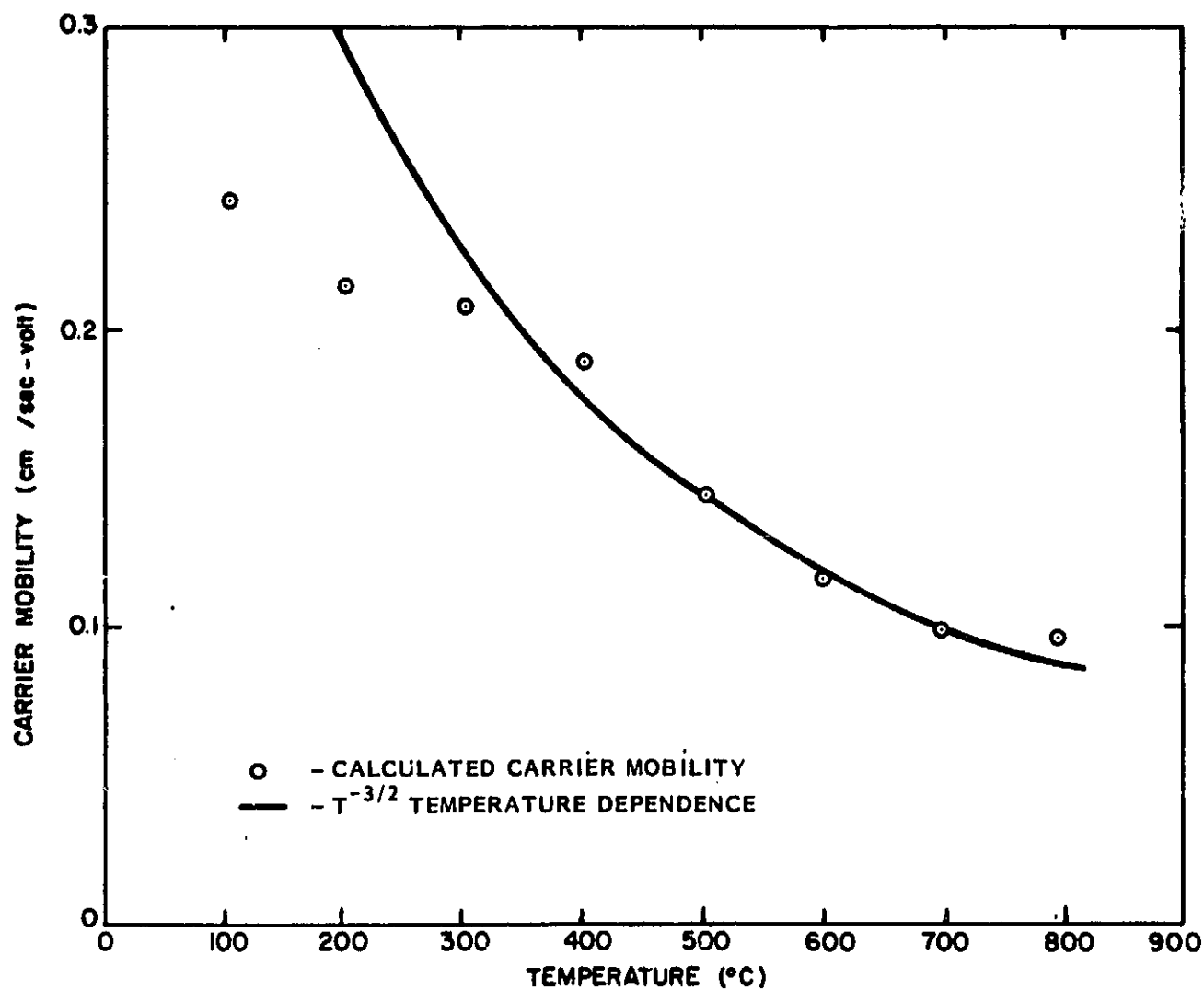


Figure 21. Carrier Mobility of  $(\text{La}_2\text{S}_3)_{0.75}(\text{Cr}_2\text{S}_3)_{0.25}$ .

## V. SUMMARY

This program has been concerned with the development of a thermoelectric material for use in thermoelectric energy conversion applications at temperatures up to 1000°C. A number of different materials have been investigated on the program. Of these materials, several have been identified as potentially useful materials. Among these materials, the most promising are silicon-germanium alloys with gallium phosphide additions and lanthanum chrome sulfide. The former material has been shown to possess values of figure-of-merit higher than those of silicon-germanium alloys. The latter material has figure-of-merit values that are comparable to those of silicon-germanium alloys and, it is believed, with further development can be shown to be significantly higher than those of silicon-germanium alloys.